Patras, June 13 2018
Conference and Cultural Center of the University of Patras

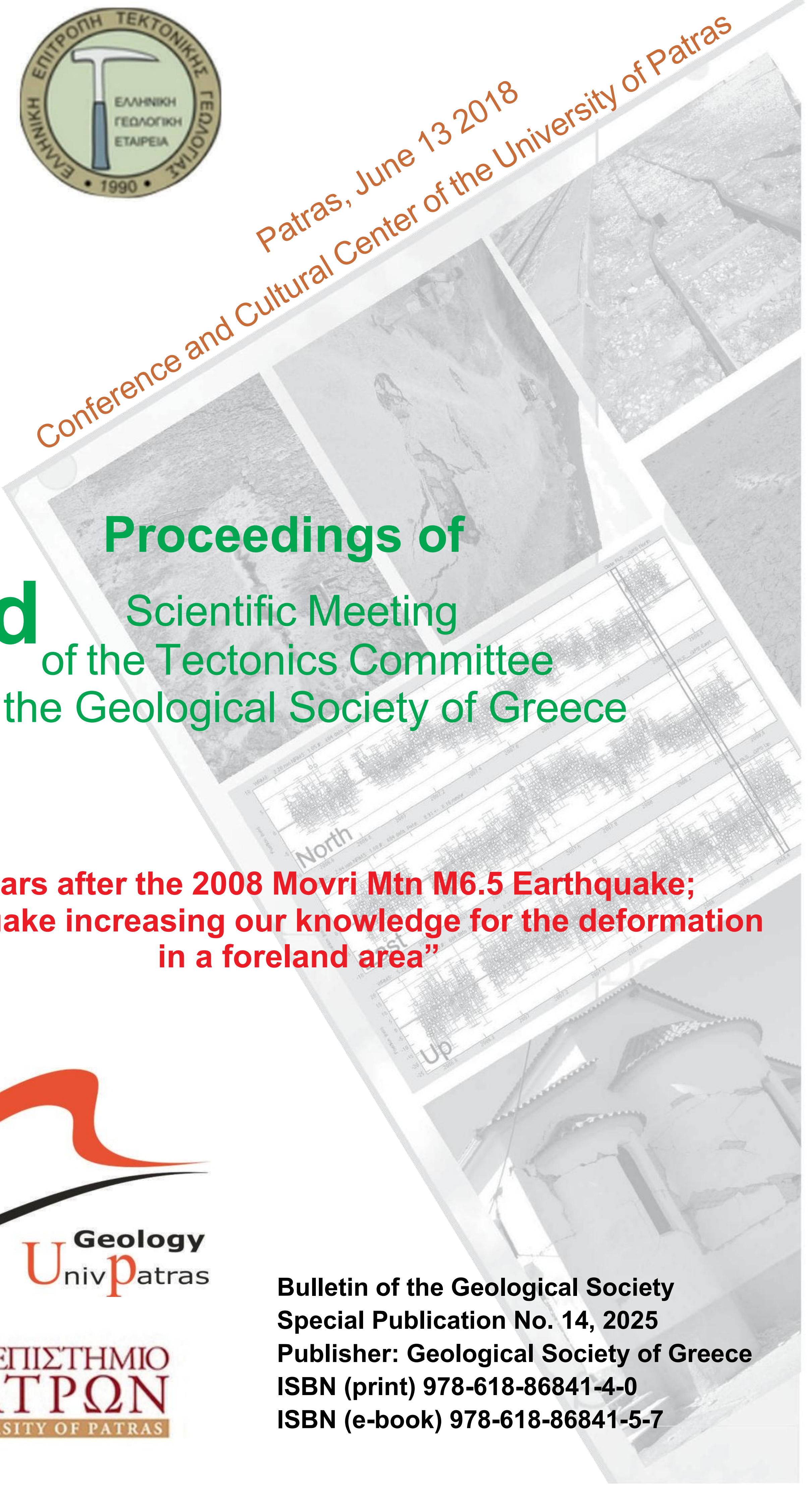

Proceedings of
2nd Scientific Meeting of the Tectonics Committee of the Geological Society of Greece

"10 Years after the 2008 Movri Mtn M6.5 Earthquake; An earthquake increasing our knowledge for the deformation in a foreland area"

Structural Geology & Tectonics
Geology UnivPatras

ΠΑΝΕΠΙΣΤΗΜΙΟ ΠΑΤΡΩΝ
UNIVERSITY OF PATRAS

Bulletin of the Geological Society
Special Publication No. 14, 2025
Publisher: Geological Society of Greece
ISBN (print) 978-618-86841-4-0
ISBN (e-book) 978-618-86841-5-7

View of the epicentral area of the Movri Mtn Earthquake

(photo courtesy Lab of Structural Geology and Tectonics)

SPONSOR OF THE 2nd SCIENTIFIC MEETING

OF THE TECTONICS COMMITTEE

OF THE GEOLOGICAL SOCIETY OF GREECE

HELLENIC PETROLEUM

Bulletin of the Geological Society
Special Publication No. 14, 2025
Publisher: Geological Society of Greece
ISBN (print) 978-618-86841-4-0
ISBN (e-book) 978-618-86841-5-7

2nd Scientific Meeting of the Tectonics Committee of the Geological Society of Greece

10 Years after the 2008 Movri Mtn M6.5 Earthquake;
An earthquake increasing our knowledge for the deformation in a foreland area

<u>Invited Speaker : Riccardo Caputo, Ferrara University (Italy)</u>

VENUE: Conference & Cultural Center of the University of Patras

Patras, 13 June 2018

Organizers

Structural Geology & Tectonics
Geology UnivPatras

ΕΛΛΗΝΙΚΗ ΓΕΩΛΟΓΙΚΗ ΕΤΑΙΡΕΙΑ – ΕΠΙΤΡΟΠΗ ΤΕΚΤΟΝΙΚΗΣ ΓΕΩΛΟΓΙΑΣ – 1990

Sponsor

HELLENIC PETROLEUM

ORGANISING COMMITTEE OF THE 2nd SCIENTIFIC MEETING

OF THE TECTONICS COMMITEE

OF THE GEOLOGICAL SOCIETY OF GREECE

PRESIDENT

Professor Ioannis Koukouvelas

Department of Geology, University of Patras

VICE-PRESIDENT

Dr. Athanasios Ganas

Institute of Geodynamics, National Observatory of Athens

SECRETARY

Dr. Vasiliki Zygouri

Department of Geology, University of Patras

MEMBERS

Associate Professor Paris Xypolias

Department of Geology, University of Patras

Dr. Charalampos Kranis

Faculty of Geology and Geoenvironment, National & Kapodistrian University of Athens

Assistant Professor Stelios Lozios

Faculty of Geology and Geoenvironment, National & Kapodistrian University of Athens

MSc Varvara Tsironi

Institute of Geodynamics, National Observatory of Athens

Dr. Emmanuel Skourtsos

Faculty of Geology and Geoenvironment, National & Kapodistrian University of Athens

MSc Sotirios Verroios

Department of Geology, University of Patras

CONTENTS

Co-seismic & inter-seismic ground deformations in the Movri earthquake area

PIERRE BRIOLE[1], PANAGIOTIS ELIAS[2], ANTONIO AVALLONE[3], DIMITAR DIMITROV[4]

[1]*Ecole Normale Supérieure / PSL Research University, UMR CNRS 8538 / Laboratoire de Géologie*
24 Rue Lhomond, 75005 Paris, France
[2]*National Observatory of Athens, Institute for Astronomy, Astrophysics, Space Applications & Remote Sensing*
Vas. Pavlou & I. Metaxa, 15236 Penteli, Greece
[3]*Istituto Nazionale di Geofisica e Vulcanologia*
Via di Vigna Murata 605, 00143 Roma, Italy
[4]*Bulgarian Academy of Sciences, National Institute of Geophysics, Geodesy and Geography,*
Acad. G. Bonchev Str. bl. 3, 1113 Sofia, Bulgaria,
briole@ens.fr, pelias@noa.gr, antonio.avallone@ingv.it, clgdimi@bas.bg

Keywords: *GPS, InSAR, elastic model*

Abstract

The co-seismic deformation associated with the Movri earthquake was measured by both GPS and SAR interferometry. Its amplitude is small for an earthquake of such magnitude occurring within the crust. Its modelling, assuming an elastic and homogeneous crust, implies that the fault tip is located at a depth greater than 10 km. The location of the fault, its NS extension and the amplitude of slip are well constrained by the data. The 2008 fault could belong to a tectonic boundary signed further north, and at shallower depth, by the Patras-Rio fault. The inter-seismic GPS data show indeed the existence of a block in the north-west Peloponnese (from Kato Achaia to Amaliada to the east to Killini to the west) with GPS velocities significantly different from that of the Peloponnese. The 2008 fault location is consistent with the eastern border of that block although the number of permanent and campaign points in the area is still not sufficient to infer accurately the boundary and the possible deformation gradients in the boundary. Measuring this gradient, i.e. inferring the location of the locked zone during the inter-seismic period would be important better understanding the deformation and stress accumulation / release processes in the area, especially in the upper crust above the tip of the ruptured zone. Is there a possibility of earthquake at shallower depth above the fault that ruptured in 2008? Or, is this upper crust deforming in a manner different from the lower crust? After the earthquake, permanent GPS stations were left during a month in the epicentre area but no significant post-seismic signal was detected.

The seismic gap of northern Thessaly, Central Greece

RICCARDO CAPUTO[1,2,3]

[1]*Department of Physics and Earth Sciences*
University of Ferrara, Italy
[2]*Centro Inteniversitario per l'analisi Sismotettonica tridimensionale*
CRUST -UR UniFE, Italy
[3]*Research and Teaching Centre for Earthquake Geology*
Tyrnavos, Greece
rcaputo@unife.it

Keywords: *seismotectonics, seismic hazard, Thessaly*

Abstract

Based on three decades of geological, morphotectonic and geophysical surveys carried out all over Thessaly, the major seismogenic faults affecting the area have been clearly recognized and mapped. Each tectonic structure has been commonly investigated on the basis of multiple Earthquake Geology approaches, including structural mapping, remote sensing analyses, morphotectonic campaigns, palaeoseismological trenches and related chronological analyses based on different methods, microtopographic profiling, archaeoseismological studies, geophysical surveys among which high resolution seismic reflection, ground penetrating radar, electrical resistivity tomographies, microtremor recording. For many of these faults, also the degree of fault activity (i.e. the long-term slip-rate) has been tentatively constrained. Accordingly, the pattern and distribution of the several investigated faults clearly reflect the active stress field affecting the broader Aegean Region including Thessaly. However, when we analyse the distribution of the instrumental seismicity, say the last century, all major events associated with magnitudes greater than M6 have occurred along the southern Thessalian sector and specifically, the Domokos (1954; M7.0), Righeo (1957; M6.5 and M6.6) and Nea Anchialos (1980 and 1985; M6.5). On the other hand, only the 1941 event (M6.1), whose real magnitude is still debated due to the IIWW affairs, has occurred in the northern sector of Thessaly. In agreement with the above information, it is suggested that northern Thessaly is characterized by a major seismic gap and the seismic hazard of the region is strongly influenced by the seismogenic potential of the existing sources.

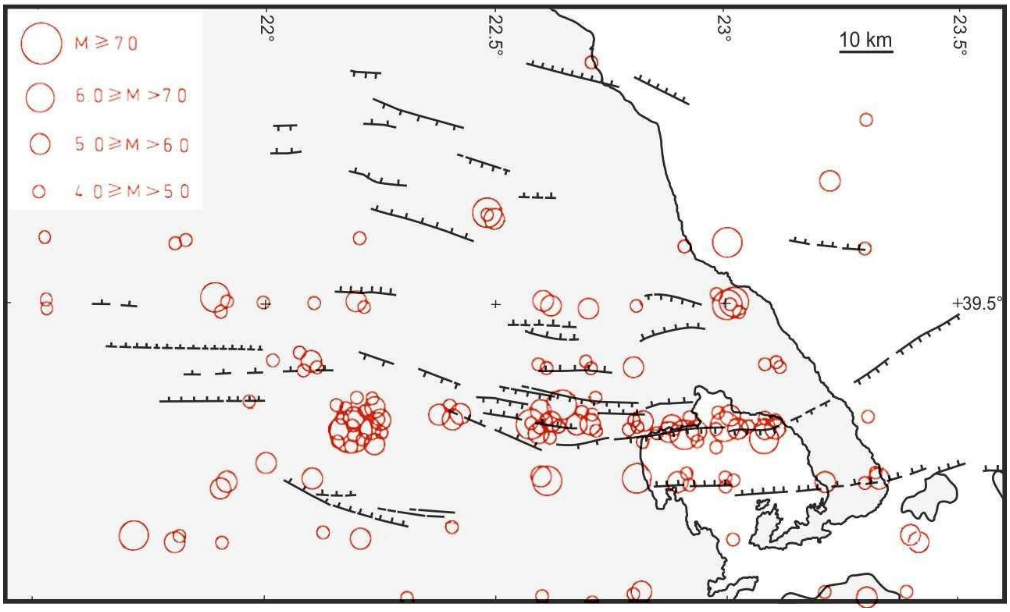

Figure 1. Major active faults affecting Thessaly (Caputo, 1995) and instrumental seismicity (Comninakis and Papazachos, 1986).

Active tectonic evidence in the NE edge of the Campania Plain, southern Apennines (Italy)

CIRO CERRONE[1], ALESSANDRA ASCIONE[1], VALENTINO DI DONATO[1], STEFANO MAZZOLI[1], GAETANO ROBUSTELLI[2]

[1]*Department of Earth, Environmental and Resources Science (DiSTAR), University of Naples Federico II*
Via Cinthia 21, 80126 Naples, Italy
[2]*Department of Biology, Ecology and Earth Science (DiBEST), University of Calabria*
Via P. Bucci, Arcavacata di Rende, Cosenza, Italy
ciro.cerrone@unina.it, ascione@unina.it, valentino.didonato@unina.it, stefano.mazzoli@unina.it, gaetano.robustelli@unical.it.

Keywords: *Raised paleoshorelines, active faults, Southern Apennines, Campania Plain, Quaternary sea-level*

Abstract

The Campania Plain is the largest coastal graben on the Tyrrhenian side of the southern Apennines. Shortening in the NE vergent southern Apennines fold and-thrust-belt was coeval, starting from the late Tortonian, with extension in the Tyrrhenian back-arc basin (Malinverno & Ryan, 1986; Patacca et al., 1990; Sartori, 1990). The eastward migration of the Tyrrhenian basin extensional front caused the drowning of the innermost part of the southern Apennines mountain belt and, starting from the Early Pleistocene, formation of large and deep basins such as the Campania Plain (Santangelo et al., 2017 and references therein). These basins are bounded towards the NW by NE-SW trending master fault systems. Data from seismic stratigraphy, geophysics and both deep and shallow boreholes (Romano et al., 1994; Barra et al., 1996; Florio et al., 1999; Cella et al., 2007; ViDEPI, 2009; Santangelo et al., 2010; Milia & Torrente, 2015) were used to reconstruct the geological evolution of the Campania Plain graben, but few surface geology data are available.

With the aim of constraining the tectonic evolution and the late Quaternary vertical motion of the northeastern boundary of the Campania Plain, a morphotectonic study of Mt. Fellino ridge was carried out by the integration of geomorphological, structural and Quaternary stratigraphy analyses, and field surveys. For the geomorphological analysis CTR 1:5000 topographic scale maps and a 5mX5m DTM were used.

The backbone of Mt. Fellino ridge is formed of carbonate rocks. The southern slope of Mt. Fellino is a ~ E-W oriented fault scarp that is characterized by a straight profile. A series of quarry cuts along that slope expose Quaternary sediments composed of shallow marine deposits bearing benthic foraminifera fauna, alluvial and pyroclastic deposits. Overall evidence shows that such deposits are related to tens of meter thick transgressive-regressive successions consisting of beach conglomerates (made up of well rounded clasts) and fossiliferous sands, which passes upwards to alluvial fan and slope deposits. The depositional successions rest on wide wave-cut terraces standing from 50 m to 200 m a.s.l.

Oblique-slip NW-SE and N-S trending extensional and transfer faults dissect the marine-continental deposits (Fig.1), which are downfaulted by ~ E-W trending normal faults beneath the Holocene alluvial plain to the south of Mt. Fellino. Based on subsurface stratigraphy data offset of the E-W trending normal faults bounding Mt. Fellino ridge to the south is at least 230 m. Some geomorphological evidence from the alluvial plain to the S of Mt. Fellino such as few metre high rectilinear scarps, the presence of marshy, ponded areas and anomalies in the drainage network suggest recent activity of the E-W trending faults.

In conclusion, the new surface data on Quaternary units along the fault scarp of Mt. Fellino have provided new data on the evolution of the northern Campania Plain. Furthermore, the new data have allowed constraining the geometry and kinematics of the faults that bound Mt. Fellino to the south, and suggest recent (late Quaternary, possibly Holocene) activity of such faults.

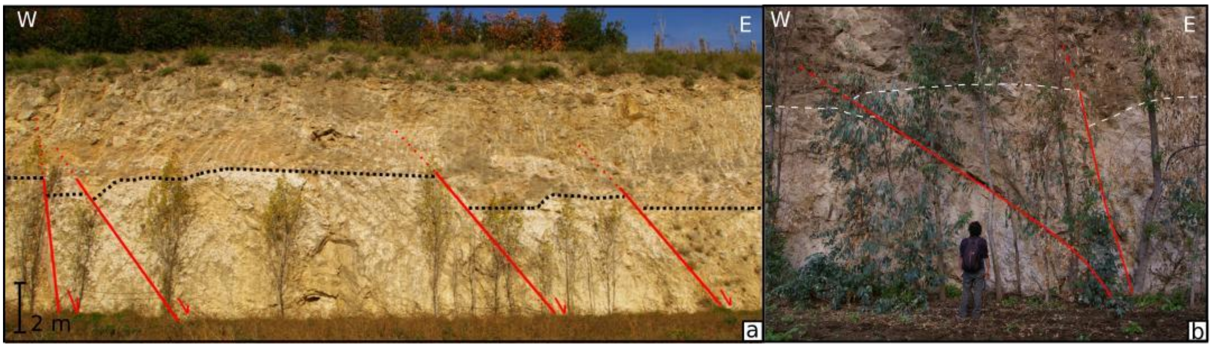

Figure 1. (a) N-S trending extensional faults which cut the wave-cut terrace and the shallow-water marine sands in the Mt. Fellino area. (b) Oblique-slip NW-SE and around N-S trending transfer faults. In a and b the faults displace the wave-cut platforms and the associated shallow-marine deposits at ~75 m on the southern slope of Mt. Fellino

References

Barra, D., Romano, P., Santo, A., Campajola, L., Roca, V., Tuniz, C. (1996). The Versilian trasgression in the Volturno river plain (Campania, Southern Italy): Palaeoenviron mental history and chronological data. Quat. 9, 445–458.

Cella, F., Fedi, M., Florio, G., Grimaldi, M., Rapolla, A. (2007). Shallow structure of the Somma-Vesuvius volcano from 3D inversion of gravity data. J. Volcanol. Geotherm. Res. 161, 303–317. https://doi.org/10.1016/j.jvolgeores.2006.12.013

Florio, G., Fedi, M., Cella, F., Rapolla, A. (1999). The Campanian Plain and Phlegrean Fields: structural setting from potential field data. J. Volcanol. Geotherm. Res. 91, 361–379. https://doi.org/10.1016/S0377-0273(99)00044-X

Malinverno, A., Ryan, W.B.F. (1986). Extension in the Tyrrhenian Sea and shortening in the Apennines as result of arc migration driven by sinking of the lithosphere. Tectonics 5, 227–245. https://doi.org/10.1029/TC005i002p00227

Milia, A., Torrente, M.M. (2015). Tectono-stratigraphic signature of a rapid multistage subsiding rift basin in the Tyrrhenian-Apennine hinge zone (Italy): A possible interaction of upper plate with subducting slab. J. Geodyn. 86, 42–60. https://doi.org/10.1016/j.jog.2015.02.005

Patacca, E., Sartori, R., Scandone, P. (1990). Tyrrhenian basin and Apenninic Arcs: kinematic relations since Late Tortonian times. Mem. Soc. Geol. It 45, 425–451. https://doi.org/10.1007/978-94-011-2016-6_7

Romano, P., Santo, A., Voltaggio, M. (1994). L'evoluzione geomorfologica della piana del fiume Volturno (Campania) durante il tardo Quaternario (Pleistocene medio-superiore-Olocene). Quat. - Ital. J. Quat. Sci. 7, 41-56.

Santangelo, N., Ciampo, G., Di Donato, V., Esposito, P., Petrosino, P., Romano, P., Ermolli, E.R., Santo, A., Toscano, F., Villa, I. (2010). Late quaternary buried lagoons in the northern campania plain (southern Italy): Evolution of a coastal system under the influence of volcano-tectonics and eustatism. Ital. J. Geosci. 129, 156–175. https://doi.org/10.3301/IJG.2009.12

Santangelo, N., Romano, P., Ascione, A., Russo Ermolli, E. (2017). Quaternary evolution of the Southern Apennines coastal plains: a review. Geol. Carpathica 68, 43–56. https://doi.org/10.1515/geoca-2017-0004

Sartori, R. (1990). The Main Results of ODP Leg 107 in the Frame of Neogene To Recent Geology of Peri-Tyrrhenian Areas. Proc. Ocean Drill. Program, Sci. Results, 107, 715–730.

ViDEPI (2009). Progetto Visibilità Dati Esplorazione Petrolifera in Italia, © 2009–2010 Ministero dello Sviluppo Economico UNMIG, Società Geologica Italiana, Assomineraria. http://unmig.sviluppoeconomico.gov.it/videpi/

A review of kinematics of west-central Greece from GNSS data: exploring the boundaries of extension and shear

ATHANASSIOS GANAS AND THE NOA GPS GROUP*
*KONSTANTINOS CHOUSIANITIS, GEORGE DRAKATOS, PANAGIOTIS ARGYRAKIS, MARIOS PAPANIKOLAOU, PANAGIOTIS ELIAS, EVANGELOS MENDONIDIS, CHRISTINA TSIMI, ALEXANDRA MOSHOU, NIKOS ROUKOUNAKIS, DIMITRIS MAKARIS, KONSTANTINOS EXARCHOS

Institute of Geodynamics National Observatory of Athens
Lofos Nymfon, Thission P.O Box 20048, 11810 Athens, Greece
aganas@noa.gr

Abstract

Geodetic data from permanent GNSS (GPS) stations in central and western Greece have been used to map tectonic deformation in this highly active region of Eurasia. The data comprise 30-s daily observations during the last two decades and have appeared in several publications by various teams (NOA, MIT, ENS, NTUA, NKUA, Oxford etc). The primary product is the crustal velocity field in the ITRF2008 and the Eurasian-fixed reference frame. In turn, the dense station distribution allows to compute 2D (horizontal) strain-rate and rotation-rate maps using the weighted least squares approach such as that of Shen et al. (JGR, 1996, 2015). The largest extension is observed in the western and central part of the Corinth rift (around 250 – 300 ns/yr) with a prominent N-S pattern that matches well both seismological and geological data. The gulf of Corinth is a young rift separating two crustal blocks of central Greece while significant strain is accumulated in its western termination. Shortening (compression) is observed over large areas of western Greece due to horizontal movements (shearing) of several crustal blocks, most important being the block abutting the Cephalonia Transform Fault (CTF). The boundary of compression in NW Peloponnese is mapped in the vicinity of the 8 June 2008 M=6.5 earthquake.The pattern of deformation fits better discontinuous (fault-driven) models than continuum motions (orogenic collapse of the Hellenides).

The seismic anisotropy pattern in the epicentral area of the 2008 Movri Mtn M6.5 earthquake

DIMITRIOS GIANNOPOULOS[1], EFTHIMIOS SOKOS[2], KONSTANTINOS KONSTANTINOU[3], ATHANASIOS LOIS[1], DIMITRIOS KONSTANTINOPOULOS[2]

[1]*Seismotech S.A.*
6 Agisilaou str, Marousi, 15123 Athens, Greece
[2]*Laboratory of Seismology, Department of Geology, University of Patras*
26504 Rio, Patras, Greece
[3]*Department of Earth Sciences, National Central University*
Jhongli 320, Taiwan
dgiannopoulos@seismotech.gr, lois@seismotech.gr, esokos@upatras.gr, dkonstantinopoulos@upatras.gr, kkonst@cc.ncu.edu

Keywords: *Seismic anisotropy; Shear-wave splitting, Stress field, Wave propagation, Crustal structure*

Abstract

The Movri Mtn earthquake (M6.5) occurred on June 8, 2008, in north-western Peloponnese, Greece, about 35km southwest of the city of Patras. It is considered as the largest instrumentally recorded seismic event in this area to date. For the purpose of this study, part of the aftershock sequence of the Movri Mtn earthquake, recorded by a portable network of six stations and a permanent station of the Hellenic Unified Seismological Network (HUSN), was analysed in order to perform a local S wave anisotropy analysis.

An indicator which is frequently used to indentify and measure seismic anisotropy, is the shear wave splitting (SWS) phenomenon. SWS occurs during S wave propagation through an anisotropic medium, as S waves are splitted into two components with perpendicular polarization directions and different propagation velocities (Crampin & Chastin, 2003). The two splitting parameters that can be measured defining the anisotropy, are the polarization direction of the fast S wave component and the time-delay between the two components.

The waveform data utilized in this study consists of aftershocks of the Movri Mtn earthquake recorded between June 14th and September 17th 2008. The hypocentral location process provided a dataset of 78 earthquakes as the input for the SWS analysis, with focal depths ranging from 7km to 25km and magnitudes from 2.3 to 3.4. The calculated mean location uncertainties were, RMS=0.12 s, ERZ=1.27 km and ERH=1.14 km.

The SWS analysis was performed using the cross-correlation (CC) method, initially proposed by Ando et al. (1983). According to the CC method, the horizontal components are rotated in the horizontal plane at 1° increment of azimuth from -90° to 90°. Then, for each azimuth, the CC coefficient is calculated between the two orthogonal seismograms, for a range of time-delays in a selected time window. When the absolute value of the CC coefficient reaches a maximum, the corresponding values of azimuth and time are chosen as the fast polarization direction and the time-delay between the splitted S waves, respectively. The seismograms used for the analysis were integrated to displacement and band-pass filtered between 1 and 10Hz. For each waveform, the start of the measurements' time window was fixed 0.05s before the S wave arrival, while the endpoint, using a step of 0.02s, was adjusted until the value of CC coefficient between the fast and slow components was maximized.

The analysis provided 200 valid splitting measurements derived from 78 seismic events. The mean time-delays, which were normalized according to the hypocentral distances, varied per station between 1.1 ±0.5 ms/km and 2.6 ±0.6 ms/km, with a mean value of 1.7 ±0.5 ms/km. The mean fast polarization varied between NNW-SSE and NNE-SSW directions, exhibiting a mean of 170° ±9°.

The Movri Mtn earthquake occurred along a pre-existing, dextral, high angle fault, with no direct surface expression, possibly formed during past tectonic processes that affected the area. The strike of the fault is about 210°, as determined by seismological means (Konstantinou et al., 2009). The azimuth of the principal compressive stress axis of the regional stress field, inferred by a stress

inversion of all available focal mechanisms in the area (Konstantinou et al. 2011), was estimated at 273°. The angle between the strike of the fault and the σ_1 of the regional stress field shows that the fault is severely misoriented compared to the regional prevailing stress field, indicating that Movri Mtn earthquake occurred within an unfavorable stress regime.

Considering that for seismogenic fault reactivation to occur, a favorable orientation between the strike of the fault and σ_1 is needed, Konstantinou et al. (2011) suggested that the presence of fluids may have facilitated the reactivation of the fault causing the 2008 event. Fluids could have allowed the fault to slip by rotating the principal stress axis locally around the fault to more favorable angles.

The polarization directions of the fast-traveling S wave components are usually parallel or sub-parallel to the present-day direction of the maximum compressive stress throughout the crust (Crampin & Chastin 2003). The mean fast polarization orientation, using the complete dataset of the present study, was measured at 170° ±9°. Thus, we can claim that the direction of the maximum horizontal compressive stress at the study area is almost parallel to this value, indicating the presence of a local stress field in the vicinity of the fault with different characteristics from those of the prevailing regional stress field. Comparing the strike of the fault (210°) and the mean fast polarization direction (170° ±9°), it seems that the local σ_1 was rotated towards lower angles to the fault.

The findings of the present work, as well as the suggestion of possible fluid involvement, is also supported by a recent SWS analysis carried out at the same area (Giannopoulos et al. 2013). In this study, a single station SWS analysis was performed by analyzing foreshocks and aftershocks of the Movri Mtn earthquake recorded at the closest available HUSN's station to the seismogenic fault. The results revealed a mean fast polarization direction of 164° ±10°, as well as a distinct increase in the time-delays soon after the occurence of the Movri Mtn earthquake.

The observations of the current analysis can be explain by the EDA and APE models (Zatsepin & Crampin, 1997), highlighting a key role for over-pressured fluids in the splitting parameters. We suggest that SWS in the epicentral area of the Movri Mtn earthquake was most probably caused by fluid-saturated micro-cracks, oriented parallel or sub-parallel to the maximum compressive stress axis of a local stress field in the vicinity of the fault. The cause of the observed differences between the fast polarization directions and the regional prevailing stress field was a possible migration of fluids through the fractured damage zone which allowed local rotations of the stress field. This suggestion could also explain to some extent, the differences between the average normalized time-delay values per station, which they possibly reflect parts of the crust with different level of deformation and micro-crack systems with different geometry (crack density and aspect ratio) and level of saturation.

References

Ando, M., Ishikawa, Y., Yamazaki, F. (1983). Shear wave polarization anisotropy in the upper mantle beneath Honshu, Japan. J. Geophys. Res., 88, 5850-5864.

Crampin, S., Chastin, S. (2003). A review of shear wave splitting in the crack-critical crust. Geophys. J. Int, 155, 221-240.

Giannopoulos, D., Sokos, E., Konstantinou, K.I., Lois, A., Tselentis, G. (2013). Temporal variation of shear-wave splitting parameters before and after the 2008 Movri Mountain earthquake in northwest Peloponnese (Greece). Annals Of Geophysics, 55(5). doi:10.4401/ag-5586.

Konstantinou, K. I., Melis, N. S., Lee, S.-J., Evangelidis C. P., Boukouras K. (2009). Rupture Process and Aftershocks Relocation of the 8 June 2008 Mw 6.4 Earthquake in Northwest Peloponnese, Western Greece. Bulletin of the Seismological Society of America, Vol. 99, No. 6, 3374-3389.

Konstantinou, K. I., Evangelidis, C. P., Melis, N. S. (2011). The 8 June 2008 MW 6.4 Earthquake in Northwest Peloponnese, Western Greece: A Case of Fault Reactivation in an Overpressured Lower Crust?. Bulletin of the Seismological Society of America, Vol. 101, No. 1, 438-445.

Zatsepin, S.V., Crampin, S., (1997). Modelling the compliance of crustal rock-I. Response of shear-wave splitting to differential stress, Geophys. J. Int., 129, 477-494.

Recent seismicity/microseismicity study in Western Peloponnese, Greece

ANTOINE HADDAD[1], MATTEO LUPI[1], THOMAS PLANES[1], ATHANASSIOS GANAS[2], IOANNIS KASSARAS[3]

[1]*Crustal Deformation and Fluid Flow Group, University of Geneva,*
Rue des Maraîchers 13,CH-1205 Genève
[2]*Institute of Geodynamics, National Observatory of Athens*
Lofos Nymfon, Thission P.O Box 20048 11810 Athens, Greece
[3]*Department of Geophysics and Geothermy, National and Kapodistrian University of Athens*
Panepistimiopolis, 15784, Athens, Greece
antoine.haddad@unige.ch, matteo.lupi@unige.ch, thomas.planes@unige.ch, aganas@gein.noa.gr, kassaras@geol.uoa.gr

Abstract

This study reports investigations on the ongoing seismicity in the Western Peloponnese, Greece. The aim is to shed light on the crustal deformation of the region. To capture the evolution of the seismic sequences we deployed a local seismic network consisting of 15 temporary (Short Period Lennartz LE-3Dlite 1s) deployed in a polygon between 39°N to 37°S and from 20°W to 22°E. The acquired data have been complemented with those from 9 permanent seismic stations of the Hellenic Unified Seismological Network (HUSN).

We recorded and located 1515 earthquakes with magnitudes ranging from ML1.1 to ML4.6 from July 2016 to May 2017. The catalogue of events was built using STA/LTA methods and then PhasePApy python package for auto-picking (Chen & Holland 2016). We used PSPicker (Baillard et al. 2014) to refine the P and S arrivals. By applying the location errors minimization technique, 1-D optimum local velocity models constraints (Haslinger 1998, Kassaras et al. 2016) all events were relocated. The velocity models show a heterogeneous crustal structure with seismicity clustering from 5 to 30km depth. Moment tensor solutions of the major events (i.e. M>3) were calculated pointing out the kinematics of the area. Focal mechanisms, in combination with the relocated microseismic activity, allowed detecting major seismogenic structures in the upper crust offshore Western Peloponnese.

References

Baillard, C., Crawford, W. C., Ballu, V., Hibert, C., Mangeney, A. (2014). An automatic kurtosis-based P-and S-phase picker designed for local seismic networks. Bulletin of the Seismological Society of America, 104(1), 394–409. doi:10.1785/0120120347

Chen, C., Holland A. A. (2016). PhasePApy: A Robust Pure Python Package for Automatic Identification of Seismic Phases. Seismol. Res. Lett., 87(6), 1384–1396, doi:10.1785/0220160019.

Haslinger, F. (1998). Velocity structure, seismicity and seismotectonics of northwestern Greece between the Gulf of Arta and Zakynthos. https://doi.org/10.3929/ETHZ-A-002025706

Kassaras, I., Kapetanidis, V., Karakonstantis, A. (2016). On the spatial distribution of seismicity and the 3D tectonic stress field in western Greece. Physics and Chemistry of the Earth, 95, 50–72. http://doi.org/10.1016/j.pce.2016.03.012

The Aftershock Sequence of the 2008 Achaia, Greece, Earthquake: Joint Analysis of Seismicity Relocation and Persistent Scatterers Interferometry

VASSILIOS KARAKOSTAS[1], KATARZYNA MIREK[2], MARIA MESIMERI[1], ELEFTHERIA PAPADIMITRIOU[1], JANUSZ MIREK[2]

[1]*Geophysics Department, School of Geology, Aristotle University of Thessaloniki*
GR54124 Thessaloniki, Greece
[2]*AGH University of Science and Technology, Department of Geoinformatics and Applied Computer Science*
Krakow, Poland
vkarak@geo.auth.gr, mmesimer@geo.auth.gr, ritsa@geo.auth.gr, kmirek@agh.edu.pl, jmirek@agh.edu.pl

Keywords: *Aftershock relocation, PSI method, displacement field, variable slip model, 2008 Achaia earthquake*

Abstract

On 8 June 2008 an earthquake of M_w6.4 took place in the north western part of Peloponnese, Greece. The main shock was felt in a wide area and caused appreciable damage along the main rupture area and particularly at the antipodal of the main shock epicenter fault edge, implying strongly unilateral rupture and stopping phase effects. Abundant aftershocks were recorded within an area of ~50 km in length in the period 08/06/2008 – end of 2014, by a sufficient number of stations that secure location accuracy because the regional network is pretty dense in the area. All the available phases from seismological stations in epicentral distances up to 140 km until the end of 2014 were used for relocation with the double–difference (DD) technique and waveform cross–correlation (CC) A quite clear 3–D representation is obtained for the aftershock zone geometry and dimensions, revealing the main rupture and the activated adjacent fault segments, SAR data processed using Stanford Method for Persistent Scatterers (StaMPS) and a surface deformation map constructed based on PS point displacement for the co–seismic period. A variable slip model, with maximum slip of ~1.0 m located at the lower part of the rupture plane, is suggested and used for calculating the deformation field which was found in adequate agreement with geodetic measurements. With the same slip model the static stress changes were calculated evidencing possible triggering of the neighboring faults that were brought closer to failure. The data availability allowed monitoring the temporal variation of b–values that after a continuous increase in the first five days, returned and stabilized to 1.0–1.1 in the following years. The fluctuation duration is considered as the equivalent time for fault healing, which appeared very short but in full accordance with the cease of onto–fault seismicity.

Structural analysis and scarp morphology of the active Pidima fault, Messinia, Greece using Terrestrial Laser Scanner and Photogrammetry

IOANNIS KARAMITROS[1], ATHANASSIOS GANAS[1], ALEXANDROS CHATZIPETROS[2], SOTIRIS VALKANIOTIS[3], ELENA PARTHENIOU[1], KONSTANTINA BETZELOU[1]

[1]*National Observatory of Athens, Institute of Geodynamics*
Lofos Nymfon, Thission P.O Box 20048, 11810 Athens, Greece
[2]*Aristotle University of Thessaloniki*
54124 Thessaloniki, Greece
[3]Koronidos Str., Trikala, Greece
yannis_karam@yahoo.com

Abstract

An extensive research was made on LIDAR and Terrestrial Laser Scanner (TLS) applications on Geosciences and various point cloud editing methodologies were tested and applied. The methods were applied on TLS & photogrammetric data surveyed during the years 2014, 2015 and 2017, along the active Pidima fault (Messinia, SW Peloponnese). The survey of 2015 offered a high-density point cloud of the fault scarp with millimeter accuracy and the 3D model could display even the smallest morphological anomalies of the plane surface creating a very close to real life representation. The structural analysis of the fault plane allowed for a detailed logging of its geometry and kinematics, such as the plane's dip and dip-direction angles, striations and corrugation size and arrangement. The obtained results agree with structural measurements in the field.

Acknowledgement: This research was funded by project ASPIDA "*Infrastructure Upgrade for Seismic Protection of the Country and Strengthen Service Excellence through Action*", project MIS-448326, implemented under the Action "Development Proposals for Research Bodies-KRIPIS."

Scenario based Seismic Risk assessment in Aigion for a repetition of the 15th June 1995 M6.4 earthquake

IOANNIS KASSARAS[1], GEORGIA GIANNARAKI[1], ZAFEIRIA ROUMELIOTI[2], DANAI KAZANTZIDOU - FIRTINIDOU[1], ATHANASSIOS GANAS[3]

[1]*National and Kapodistrian University of Athens, Department of Geology and Geoenvironment, Division of Geophysics-Geothermics*
Panepistimiopolis, Zografou, Athens 15784, Greece
[2]*Aristotle University of Thessaloniki, Department of Civil Engineering*
Thessaloniki 54124, Greece
[3]*National Observatory of Athens, Institute of Geodynamics*
Athens 11810, Greece
kassaras@geol.uoa.gr, gettegian@gmail.com, dkazantzidou@geol.uoa.gr, zroum@auth.gr, aganas@noa.gr

Keywords: *Seismic Risk, Seismic Hazard, Macroseismic Vulnerability, HVSR, Stochastic Simulation*

Abstract

Aigion city is situated at the western Corinth Gulf in Central Greece, an asymmetric graben, and one of the fastest continental rifts globally, opening at a rate of 15 cm/yr. This structure is formed by both onshore and offshore en-échelon E-W striking normal faults, north-dipping at the southern part of the rift, and south-dipping at the northern part (Fig. 1a). A large number of strong earthquakes has been reported in this area for both the historical and instrumental period. The latest destructive earthquake that caused human casualties and severe collapses is the 15th June 1995 event with **M**6.4 which occurred offshore on a shallow dipping normal fault (Bernard et al., 1997). After the earthquake, extended reconstruction works were performed and numerous damaged buildings were rehabilitated or replaced by new ones obeying to the newest rigorous seismic code of 1995.

In this work, given the high seismic hazard of the region, the short recurrence period of strong earthquakes in the Corinth Gulf, and taking advantage of new damage and geophysical data obtained after the 1995 earthquake we investigate the behavior of the present building stock of Aigion in case of repetition of the 1995 earthquake.To this aim, deterministic seismic hazard and empirical structural vulnerability are combined.Stochastic ground motion simulation was applied at 28 locations in Aigion for which free-field ambient noise measurements were available from the ASPIS-KRIPIS project; their HVSR are applied herein as proxies for the site amplification. Structural vulnerability is estimated per building through census data and detailed in-situ inspection using the empirical RiskUE-LM1 approach (Milutinovic & Trendafilloski, 2003). EMS-98 damage grades and their probabilies of occurrence were assessed by implementing the method of Giovinazzi & Lagomarsino (2004).

Structural vulnerability of Aigion was estimated for the period prior to the 1995 earthquake and the present one (2016) per building in terms of the most probable vulnerability index $\overline{V_I}$ using also modification scores, and its average is presented in a building block scale in Fig. 1b-d. Fig. 1b presents the current average $\overline{V_I}$ ranging from 0.3 (best) to 0.74 (worst), with the majority of blocks presenting $\overline{V_I} < 0.5$, while panels (c) and (d) of Fig. 1 present the EMS-98 vulnerability classes per building block prior to 1995 and for the present stock, respectively, implying a significant improvement of the state of buildings after 1995, due to rehabilitation of damaged and replacement of collapsed structures.

The enhancement of the building stock is inferred also by the comparison of the real damage due to the 1995 earthquake (Fig. 1e) and the estimated 1995 scenario-based EMS-98 damage grades (from 0 to 6) with the maximum probability to occur (Fig. 1f). As it can be seen, while in 1995 moderate-to-heavy damage was extensive in the central and the western part of the city, registered as 'need of repair' and 'unsafe for use' buildings, only slight-to-moderate damage is expected in case of repetition of this earthquake. Expected moderate effects concern old buildings mainly located at the harbor, being the ones which survived the 1995 earthquake. Although the presented model is open to improvements, it provides realistic results that highlight its usability in a prevention phase of the disaster management framework, and a future near real-time damage assessment system for the target site.

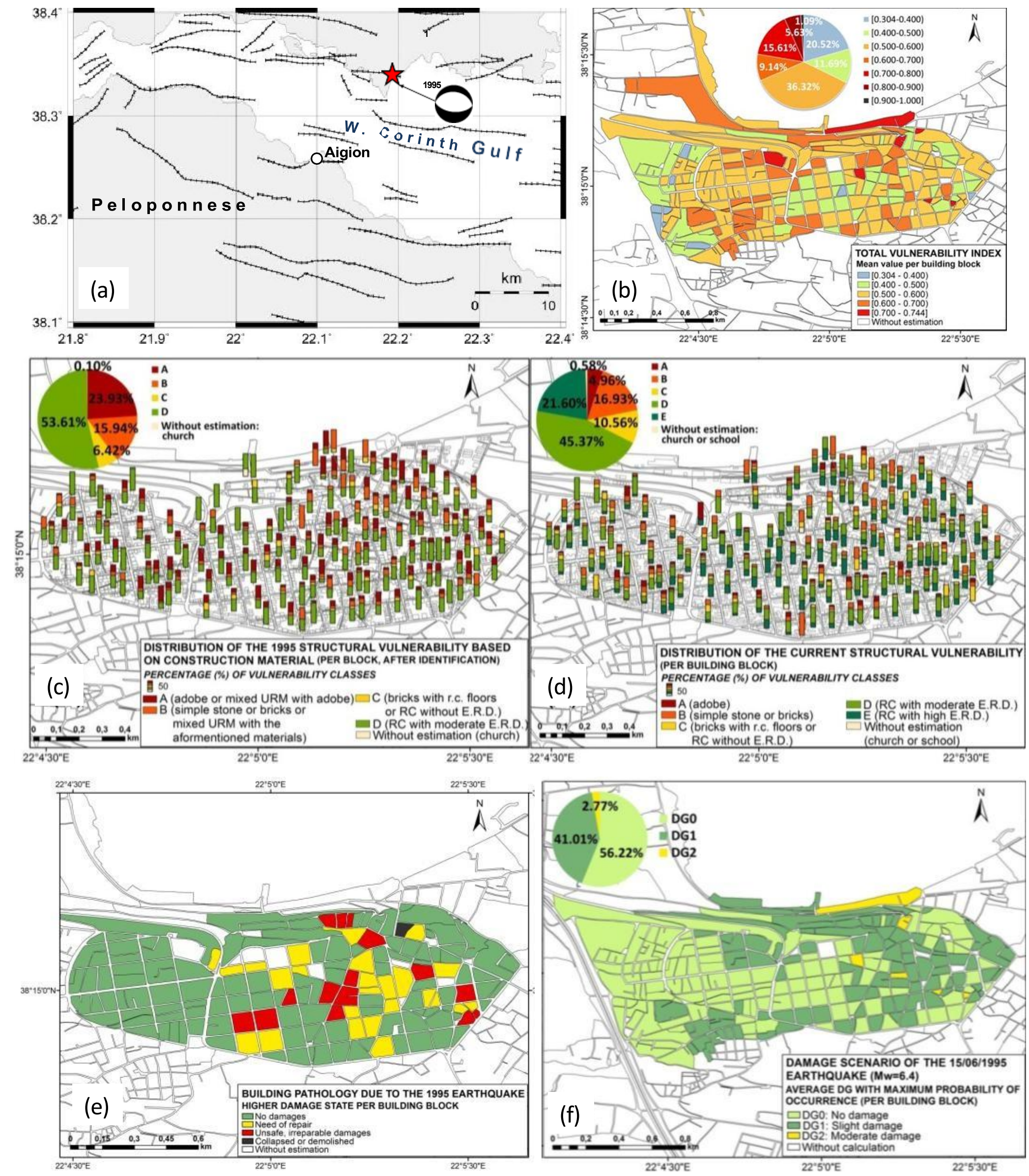

Figure 1. (a) Map presenting active faults in the western Corinth Gulf (Ganas et al., 2013), the epicenter and focal mechanism of the 1995 eq., (b) Average $\overline{V}_I$ per building block and percentage (embedded pie-chart), (c) EMS-98 vulnerability classification of the Aigion building stock before 1995, and (d) Current vulnerability classification,(e) Real damage distribution due to the 1995 earthquake with regard to prevailing damage state percentage, (f) Distribution of average EMS-98 buildings' damage grades per building block with maximum probability of occurrence in Aigion for the 1995 earthquake scenario, and percentages (embedded pie-chart).

References

ASPIS-KRIPIS (2015). Infrastructure Upgrade for Seismic Protection of the Country and Strengthen Service Excellence through Action, Project MIS-448326, implemented under the Action, Development Proposals for Research Bodies, (in Greek).

Bernard, P., et al. (1997). The Ms=6.2, June 15, 1995 Aigion earthquake (Greece): evidence for low angle normal faulting in the Corinth rift. Journal of Seismology, 1, 131–150.

Ganas, A., et al. (2013). NOAfaults: a digital database for active faults in Greece. Bulletin of the Geological Society of Greece, Proceedings of the 13th International Congress, Chania, Sept. 2013, XLVII, DOI: http://dx.doi.org/10.12681/bgsg.11079.

Giovinazzi, S., Lagomarsino, S. (2004). A macroseismic method for the vulnerability assessment of buildings. Proceedings of the 13th WCEE, Vancouver, B.C., Canada, August 1-6, No. 896.

Milutinovic, Z., Trendafilloski, G. (2003). An advanced approach to earthquake risk scenarios with applications to different European towns. Report WP4: Vulnerability of current buildings, RISK-UE, European Commission, Brussels.

The 26th March 1993 (M5.4) Pyrgos earthquake on the western segment of the Movri causative fault of the 2008 event

DANAI KAZANTZIDOU-FIRTINIDOU, IOANNIS KASSARAS, VASILIS KAPETANIDIS, ANDREAS KARAKONSTANTIS, PANAYOTIS PAPADIMITRIOU, GEORGE KAVIRIS

National and Kapodistrian University of Athens, Department of Geology and Geoenvironment, Division of Geophysics-Geothermics
Panepistimiopolis, Zografou,Athens 15784, Greece
dkazantzidou@geol.uoa.gr, kassaras@geol.uoa.gr, vkapetan@geol.uoa.gr, akarakon@geol.uoa.gr, ppapadim@geol.uoa.gr, gkaviris@geol.uoa.gr

Keywords: *Western Greece, strike-slip faulting, damage distribution, macroseismic intensities*

Abstract

This moderate sized **M**5.4 earthquake occurred on 26th March 1993, with epicentre in the Kyparissiakos Gulf, around 50 km to the east of the northwestern tip of the Hellenic Arc, near the city of Pyrgos. This area was notable for its historical paucity of large earthquakes (Fig. 1a) with the largest magnitude of the onshore seismicity being ML~5.2, until the occurrence of the **M**6.5 Movri earthquake on 8thJune 2008.The region is a transition zone, between NE-SW strike-slip tectonics and E-W normal faulting, whereas it is suggested to be situated above the tip of the Hellenic Subduction (Fig. 1b). The mainshock was widely felt,it was preceded by significant foreshock activity and was followed by numerous aftershocks. This event triggered several landslides along fault scarps and steep slopes, soil liquefaction and subsidence at the coastal area as well as several ground fractures.

The complexity of the local fault systems made it difficult to identify the causative fault, therefore vague and controversial interpretations were carried out. According to Papanastassiou et al. (1994), Stavrakakis (1996) and the GCMT Project, the main-shock displays a dextral strike-slip mechanism with a thrust component on a nodal plane striking NE-SW and dipping SE. On the contrary, Melis et al. (1994) interpret the 1993 event as occurring on a NW-SE trending, sinistral strike-slip fault-plane , due to its epicentral location falling to the south-east of the city of Pyrgos, where this orientation represents the dominant trend of faulting. These contrasting views result from the complexity of the deformation in the area (Fig. 1c-e). Nevertheless, the 2008 **M**6.5 Movri earthquake shed light to the controversies, revealing that the western segment of the ruptured NE-SW dextral strike-slip fault was most probably the causative fault of the 1993 Pyrgos earthquake.

Recorded ground motions and their resulting spectral accelerations were particularly high, in contrast with the moderate seismic coefficients with which the largest ratio of the building stock has been designed. Almost 50% of the masonry building stock was reported to be damaged; few Reinforced Concrete buildings to their bearing system, churches, neoclassical buildings of the 19th century, schools and the hospital were also impacted. The registered effects (Fig. 1f) led to intensity VIII at the town of Pyrgos (Fig. 1g). One death, few injuries and economic loss of the order of 170 M € allocated to financial aid to the affected population and rehabilitation of the town, was the aftermath of the moderate, yet damaging earthquake of 1993 in this historically active seismic area.

Study of the seismic ground response into different soil profiles by Karantoni & Bouckovalas (1997) and correlation with the spectral content of the ground motion allowed for the identification of site effects and resonance of buildings with soil sediments as possible factors influencing the spatial distribution of damage. Directivity effects are not explicitly documented, given the lack of waveform analysis; however, they are suspected because of the migration of aftershocks to the NE, the shape of the main shock intensity contours and the damage distribution.

While a debate has been recently initiated in Greece regarding the possible connection between the observed seismicity and hydrocarbon exploration and extraction in the already seismically active area of Pyrgos and western Greece, the lack of scientific publications to support it, the inherent high levels of tectonic seismicity in the area and the lack of reference to the 1993 earthquake within the Human-Induced Earthquake Database (2017) suggest that a natural origin is the most likely.

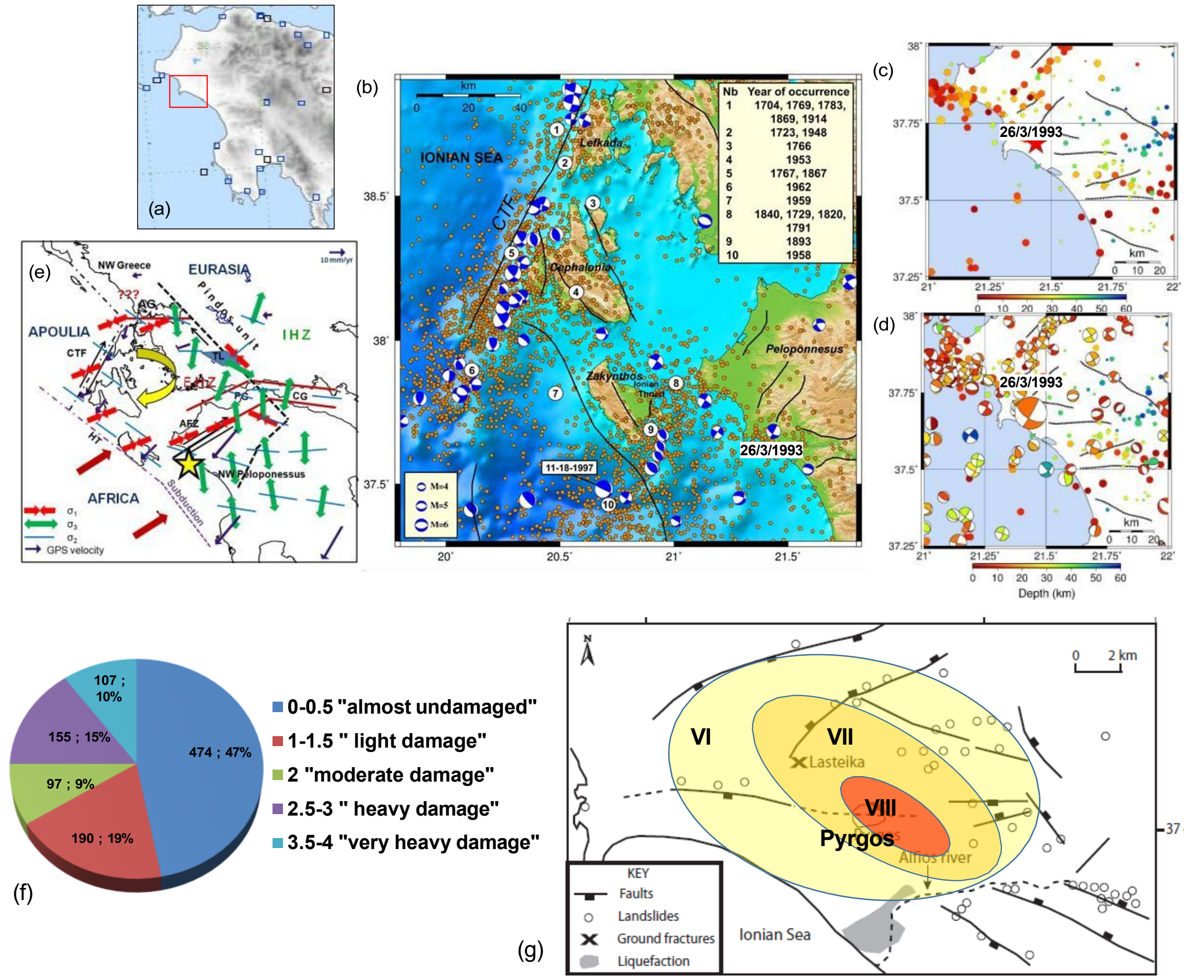

Figure 1. (a) Historical earthquakes in the broader region (AHEAD platform), (b) Seismotectonic map presenting relocated seismicity and focal mechanisms. White circles denote the most important earthquakes in the area prior to 1964 (Papadimitriou et al., 2012), (c) hypocentral locations from manually picked P- and S-wave phases (DGGSL-NKUA) (d) earthquakes as in panel c and focal mechanisms available for the area. (e) Sketch map which summarizes seismological and CGPS data: AFZ-Andravida Fault Zone; AG-Amvrakikos Gulf; CFT-Cephalonia Transform Fault; CG-Corinth Gulf; EHZ-External Hellenides Zone; HT-Hellenic Trench; IHZ-Internal Hellenides Zone; PG-Patras Gulf; TL-Trichonis Lake. The yellow star denotes the location of the 1993 earthquake, (f) Number and percentage of damaged masonry buildings per damage grade (data from Karantoni & Bouckovalas, 1997), (g) Intensity distribution in EMS-1992 scale in the broad area (modified from Lekkas et al. 2000)

References

Human Induced Earthquake Database (2017): http://inducedearthquakes.org/
Global Centroid Moment Tensor Project (GCMT): http://www.globalcmt.org
Karantoni, F., Bouckovalas, G. (1997). Description and analysis of building damage to Pyrgos, Greece earthquake. Soil Dynamics and Earthquake Engineering 16, 141-150.
Lekkas, E. et al. (2000). Intensity distribution and neotectonic macrostructure Pyrgos earthquake data (26 March 1993, Greece). Natural Hazards 21, 19–33
Melis, N. et al. (1994). The Pyrgos (March 26, 1993; Ms = 5.2) Earthquake sequence as it was recorded by the Patras seismic network. BGSG, 30(5), 175-180. Proc. 7th Congress, Thessaloniki, May 1994.
Papanastasiou, D. et al. (1994). A study of the March 26, 1993 Pyrgos (W. Peloponnese, Greece) earthquake sequence. Proc. 1992–1994, ESC, XXIV General Assembly, Athens, 451–460.
Stavrakakis, G. N. (1996). Strong motion records and synthetic isoseismals of the Pyrgos, Peloponnisos, southern Greece, earthquake sequence of March 26, 1993. PAGEOPH, 146, 147–161.

Source properties of engineering significance: examples from recent strong earthquakes in the Aegean Sea and the surrounding lands

ANASTASIA KIRATZI

Aristotle University of Thessaloniki, Department of Geophysics
54124 Thessaloniki, Greece
kiratzi@geo.auth.gr

Abstract

During the last decade (2008-2018) a cascade of strong Mw>6 earthquakes occurred in the Aegean Sea and the surrounding lands. The cluster of these events in space and time supports the ideas of earthquake interaction as a significant component of the seismic cycle. The improvement of the regional networks in Greece and Turkey and the availability of digital waveforms that span a broad spectrum of the seismic motion, provide a unique opportunity to study the characteristics of the source and the kinematics of the rupture. These studies are of paramount significance and shape the damage pattern of each strong earthquake.

The recent earthquakes which occurred in the cross border region between Turkey and Greece and affected the islands of Lesbos and Kos in Greece are unique examples to explain the large scale earthquake interaction and the source and site properties which played a role in the distribution of the damage. These ideas will be discussed and presented in view of modern ideas about the seismic cycle.

Earthquake triggered rock – falls and taluses: the case of the Skolis Mtn, North Peloponnese, Greece, before and after 2008 M6.4 earthquake

IOANNIS KOUKOUVELAS AND THE UP SGT GROUP*
ASPASIA LITOSELITI, VASILIKI ZYGOURI, SOTIRIOS VERROIOS, NIKOLAOS GEROGIANNIS, EIRINI ARAVADINOU, KONSTANTINOS NIKOLAKOPOULOS, PARIS XYPOLIAS

University of Patras, Department of Geology
26500 Rion-Patras, Greece
iannis@upatras.gr

Keywords: *Rock-falls, Earthquake triggered rock-falls, Hazard zonation, NW Peloponnese, Greece*

Abstract

The evolution of rock-falls through time and during earthquakes is considered as a useful tool to document and analyze primarily rock-falls with the intent to quantify the hazard posed by rock-falls in Greek mountainous areas prone to landslides and earthquakes. The main purpose for investigating the rock-falls associated with the Movri earthquake is to determine the landslide state of activity and geometry. The influence of the 08th June 2008 Movri earthquake, in northwestern Peloponnese, was evaluated by using aerial photographs and surface mapping in Skolis Mtn (Fig. 1). The 2008 Movri Mtn earthquake M6.4 was the most destructive of the area, affecting the NW Peloponnese and impact serious ground hazards (surface ruptures, liquefactions, rock-falls) and extensive damage to buildings along a 30 km long and 20 km wide area.

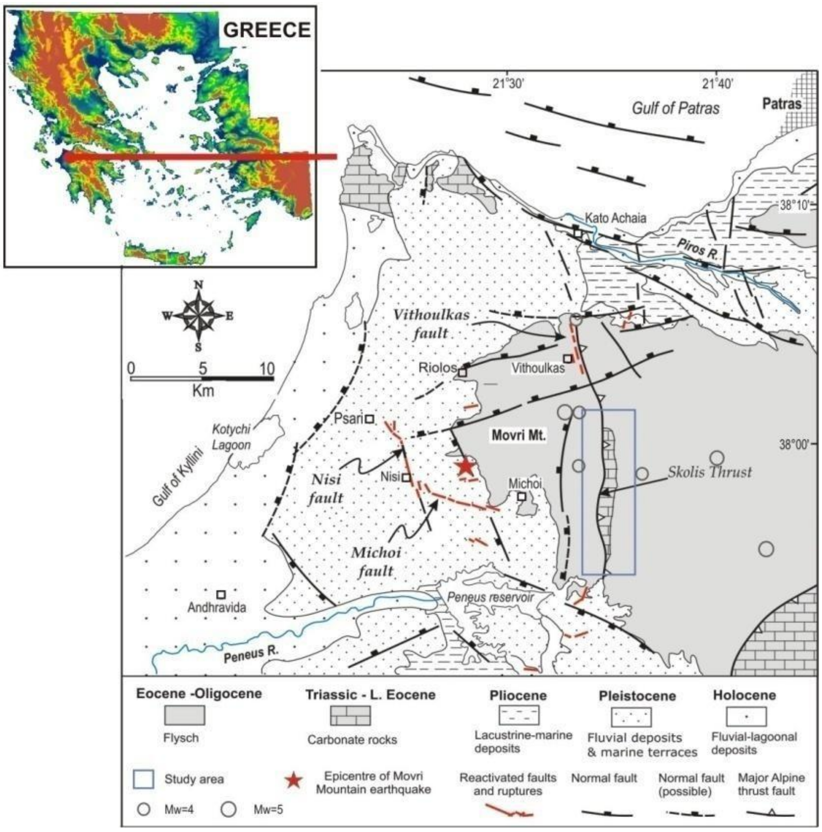

Figure 1. Map of the studied area showing lithology, active faulting and surface ruptures of the 2008 earthquake. The seismic sequence after the 2008 earthquake is reproduced from www.gein.noa.gr.

Figure 2. Steep rock cliffs of the Skolis Mtn (left image) and Helicopter post earthquake views of rock-falls and taluses (central and right images).

88 rock-fall sites were selected to estimate the hazard assessment of the earthquake. Furthermore, we remotely sensed these rock-fall sites over a large time period i.e from 1945 until 2017. In this period we recognized that the rock-falls increase their width, or their length. The terms of width and length are defined along strike or down slope the Skolis Mtn respectively. We present an outline of generating rock-fall hazard map based on rock-fall inventory and GIS. The multi-year aerial photographs helped to build a rock-fall inventory and evaluate the mass movement hazard and the morphological changes as a result of the seismic activity occurred in the last 70 years in Skolis Mtn region.

The 2008 earthquakes triggered extensive rock-falls and the fall of large blocks up to of 20 m^3. Some isolated boulders reached more than 650 m from the front scarp to the valley west of the Skolis Mtn. The most important factor determining the distance travelled by these blocks was the slope gradient, since all rolling blocks stopped where the slope gradient reached 24^o. Our intent is to highlight the role of earthquake triggered over climate-driven rock-fall phenomena, two cross-cutting but traditionally unrelated fields. This paper shows that the two processes have much in common and considerable synergism in producing harmful results of social and economic importance.

In conlusion, tectonic deformation and slope relief of Skolis Mtn play significant role in the occurrence of rock slope instabilities. Overall, post earthquake mapping shows significant size changes in rock-fall sites, while new ones are formed (Fig. 2). Therefore, the rock-fall hazard produced for the villages at the lowland of Skolis Mtn cannot be ignored.

Tracing the impact of the 2008 Movri (Ilia) Earthquake through InSAR Ground Deformation Monitoring: implications for the ESI scale

STEFANOS LAPPAS[1], MICHAEL FOUMELIS[2], IOANNIS PAPANIKOLAOU[1]

[1]*Laboratory Mineralogy-Geology, Section of Geological Sciences, Department of Natural Resources and Agricultural Engineering, Agricultural University of Athens*
Iera Odos 75, 11855, Athens, Greece
[2]*BRGM – French Geological Survey, Risk and Prevention Department*
3 avenue Claude Guillemin, BP 36009, 45060 Orléans, France
steflappas@gmail.com, i.pap@aua.gr, m.foumelis@brgm.fr.

Keywords: *DInSAR, SBAS, ESI Scale, Ilia, Movri, Andravida*

Abstract

Spaceborne Synthetic Aperture Radar (SAR) interferometry has been proven as a valuable imaging geodetic tool for measuring ground deformation over large areas. In the present study, time series of ground deformation obtained through SAR interferometry has been used in order to detect and monitor the effects of the 2008 Movri earthquake that affected a significant part of the Ilia prefecture.

Differential SAR Interferometry (DInSAR) technique exploits the phase difference of two SAR images acquired at different times over the same focus area. Conventional DInSAR is limited by temporal and geometrical decorrelation, due to land cover changes, as well as phase delays introduced by atmospheric contribution. Multi-temporal interferometric techniques overcome limitations encountered in single differential interferograms, as the utilization of long SAR time series allows significant compensation of the atmospheric phase component. Many different techniques have been developed for processing multi-temporal SAR data stacks. The Small BAseline Subset (SBAS) method uses multi-master interferometric pairs of short temporal separation and small perpendicular baseline in order to reduce the effects of spatial and temporal decorrelation. It is particularly valuable for processing long series of SAR imagery over areas characterized by non-linear ground deformation and provide apart from annual deformation rates, the detailed displacement histories of point-like targets.

Interferometric processing was applied through the European Space Agency (ESA) hosted processing infrastructure, named Grid Processing On Demand (G-POD). The platform offers to authorized users the ability to apply interferometric analysis (including SBAS) on a cloud computing environment. Overall, a set of 62 C-band ENVISAT SAR Single Look Complex (SLC) VV-polarization images were analyzed, covering a 9-year period from 2002 to 2010. Out of the total set, 27 acquired along the ascending orbit (track 186) and 35 along the descending orbit (track 279). From the available set of acquisitions along the satellites ascending and descending orbit, 42 images were singled out and 116 interferograms were computed. Interferometric pairs were selected with a perpendicular baseline smaller than 300 m and a maximum time span of 3 years. The choice of the reference point is one of the most important part of the analysis, as final deformation rates can vary greatly based on that selection. The reference point was selected towards the eastern part of the study area, at the limestones of the Lapithas Mountain in the Gavrovo – Tripoli Geotectonic Unit, that offers a high quality base point in terms of coherence (e.g. no vegetation) and stable bedrock overtime.

Results are provided at a ground resolution of 80x80m, offering a relatively high spatial resolution. A sufficient number of high coherence values were obtained towards the northern part of the study area. Most of the targets are concentrated over residential areas (small villages etc.), while few others correspond to isolated scatterers within densely vegetated regions. The majority of the point targets in the vicinity of the Andravida basin show subsidence, relative to the reference point, between 1.0-2.5 mm/yr, while very few exhibit uplift <1.0 mm/yr. It is interesting to note that over the 9-year period of observation, a couple of cm of subsidence have been recorded simultaneously in 7 sites towards the northern part of the study area (three of them are displayed in Figure 1 below), presenting a clear

offset on the time series. They were all recorded between 16/12/2007 and 13/7/2018. During this time period the 2008 Movri earthquake occurred. Given the magnitude of the offset compared to the overall variability of the displacement histories, its attribution to the co-seismic ground motion is a reasonable assumption.

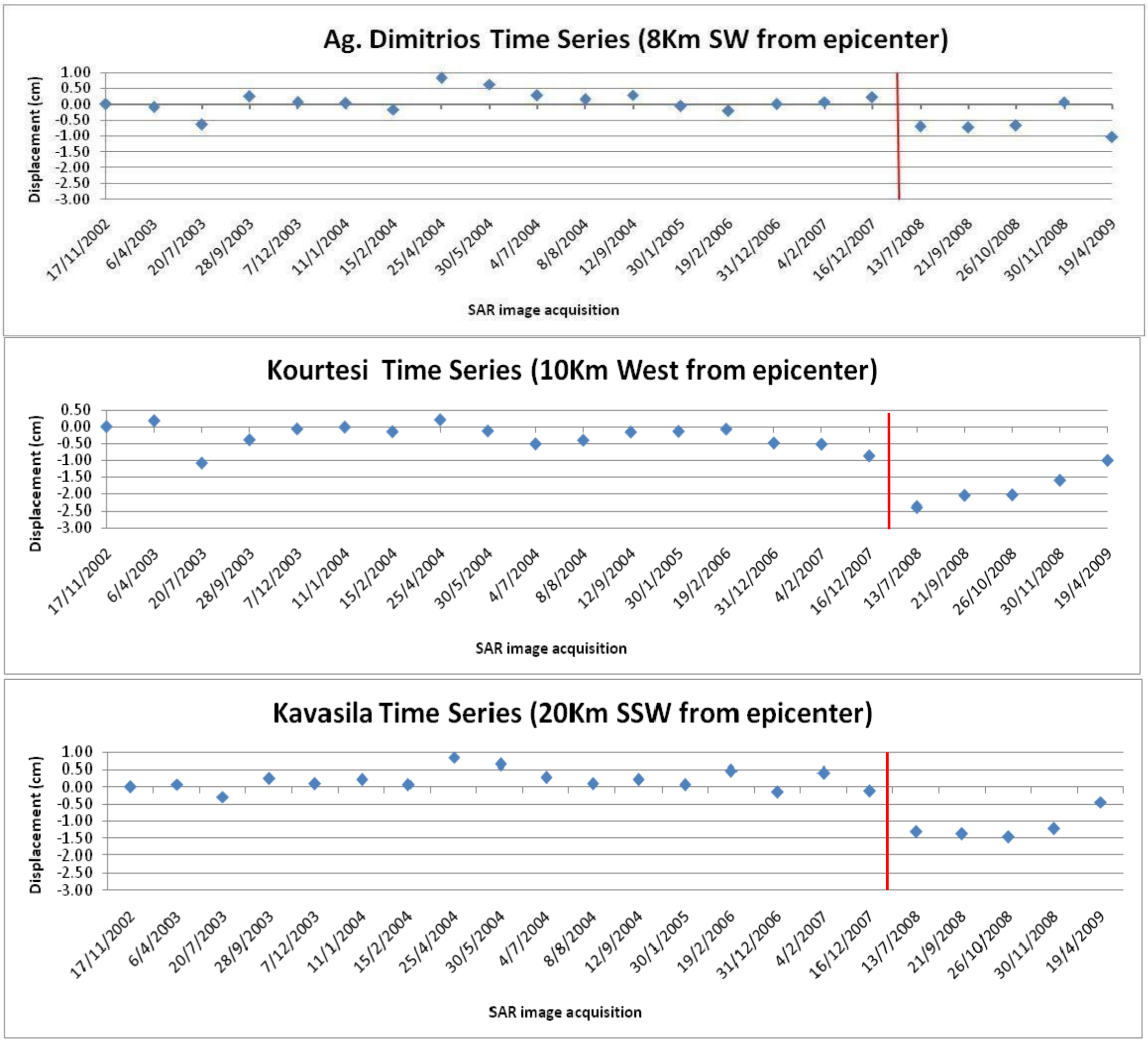

Figure 1.Time series diagrams showing the effect of the 2008 Movri earthquake in three different sites.

It is worth noticing that these displacements are recorded up to 22 km west from the epicenter of the 2008 Movri earthquake. Such recordings can be used in order to trace the extend of the EEE (Earthquake Environmental Effects) and provide more data on the ESI scale (Environmental Intensity Scale). This is particularly important for intensities VI and VII where the sensitivity of the scale is relatively poor due to the threshold on the observation of the environmental effects, implying that it is more difficult to extract field data for these intensity degrees. Therefore, this technique can help us reconstruct the deformation field and map the spatial distribution of the EEE even for a couple of cm of subsidence.

Tectonics of the Corinth Gulf, Greece, based on primary geodetic data

ILIAS LAZOS[1], ALEXANDROS CHATZIPETROS[1], SPYRIDON PAVLIDES[1], STYLIANOS BITHARIS[2], CHRISTOS PIKRIDAS [2]

[1]*Aristotle University of Thessaloniki, School of Geology, Department of Geology*
[2]*Aristotle University of Thessaloniki, School of Rural and Surveying Engineering, Department of Geodesy and Surveying*
University Campus 541 24, Thessaloniki, Greece
ilialazo@geo.auth.gr, ac@geo.auth.gr, pavlides@geo.auth.gr, smpithar@topo.auth.gr, cpik@topo.auth.gr

Keywords: *active tectonics, extensional regime, geodetic data, GPS stations, Corinth Gulf*

Abstract

The WNW–ESE trending Corinth Gulf, Greece, is the most tectonically active rift in Mediterranean region, presenting extension values ranging between 7 and 16 mm/yr. A series of E–W to NW–SE active fault zones have been documented in the Corinth Gulf area, while some active fault segments appear onshore. In the southern part of Corinth Gulf, active fault zones, dipping to the north, are recorded, while the northern part is characterized by active fault zones, dipping to the south. These two groups of active fault zones confirm the rift regime of the Corinth Gulf area. Based on the Greek Database of Seismogenic Sources (GreDaSS), 15 different active individual seismogenic sources (fault zones) are recorded in the Corinth Gulf region, while the majority of seismic faults, related to historical earthquakes, are located mainly along its southern margin. The monitoring of the Corinth Gulf rift is carried out by 14 different permanently installed GPS stations, recording the margins movement. The raw data of every three stations is combined each time and a series of parameters is calculated, based on the triangle formed by these three stations. Totally 26 such triangles were extracted, while the aforementioned series of parameters is calculated for the triangle centroids, representing the triangles.

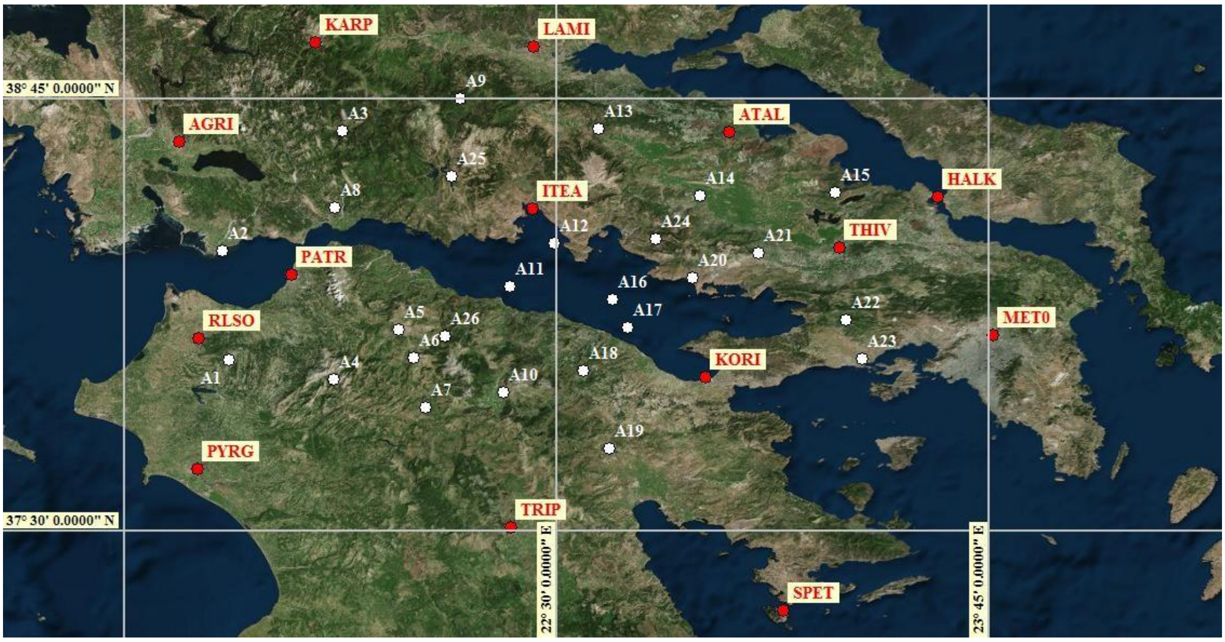

Figure 1. GPS stations (red dots) and triangle centroids (white dots) of the study area

The estimated parameters are: maximum horizontal extension, total velocity, maximum shear strain, area strain and rotation. Initially, the maximum horizontal extension rates show N–S direction, perpendicular to the fault's strike, being in agreement with the recorded fault zones. The highest values (in nano-strains) are observed into the Corinth Gulf area (A_8 = 341.47, A_{12} = 312.15, A_2 =

247.17), while the values decrease, as the distance from Corinth Gulf increases. Total velocity is estimated by the combination (Pythagorean Theorem) of North and East velocity components, presenting NE – SW direction. The total velocities have been calculated with respect to the Eurasia fixed reference frame (European Terrestrial Reference Frame 2000), confirming the NE – SW direction. The total velocity values range between 15.16 and 30.11 mm/yr, while the lowest are observed at the northeastern part and the highest at the southwestern part of the study area.

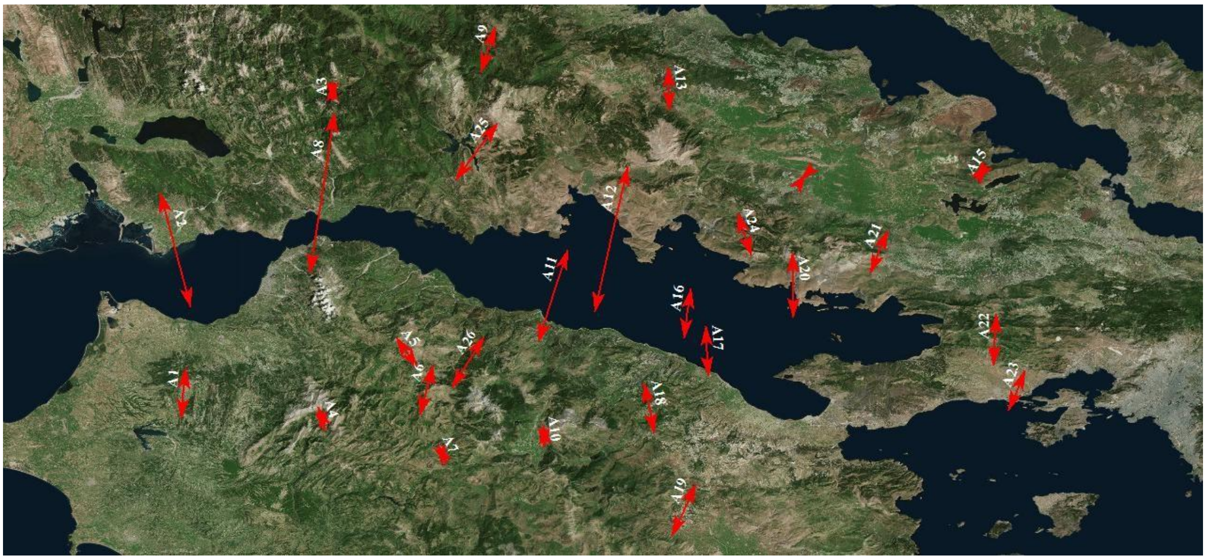

Figure 2. Maximum extension rates of the study area

Maximum shear strain is an indicator of active faulting. The highest values (in nano-strains) are concentrated into the close Corinth Gulf area (A_2 = 402.60, A_8 = 348.66, A_{12} = 326.46), as in maximum horizontal extension. Area strain shows the surface deformation (dilatation and contraction) of an area, associated with normal faulting or thrusting. The majority of the triangle centroids (approximately 85%) receive positive values, while limited negative values are observed, mainly at the southeastern part of Corinth Gulf. Negative values are interpreted as contraction the area and therefore the presence of tectonic features, related to compression (thrusts or strike-slip faulting) is possible. The positive area strain values range between 10.65 and 334.29 nano-strains and the negative between -3.02 and -137.73 nano-strains, respectively.

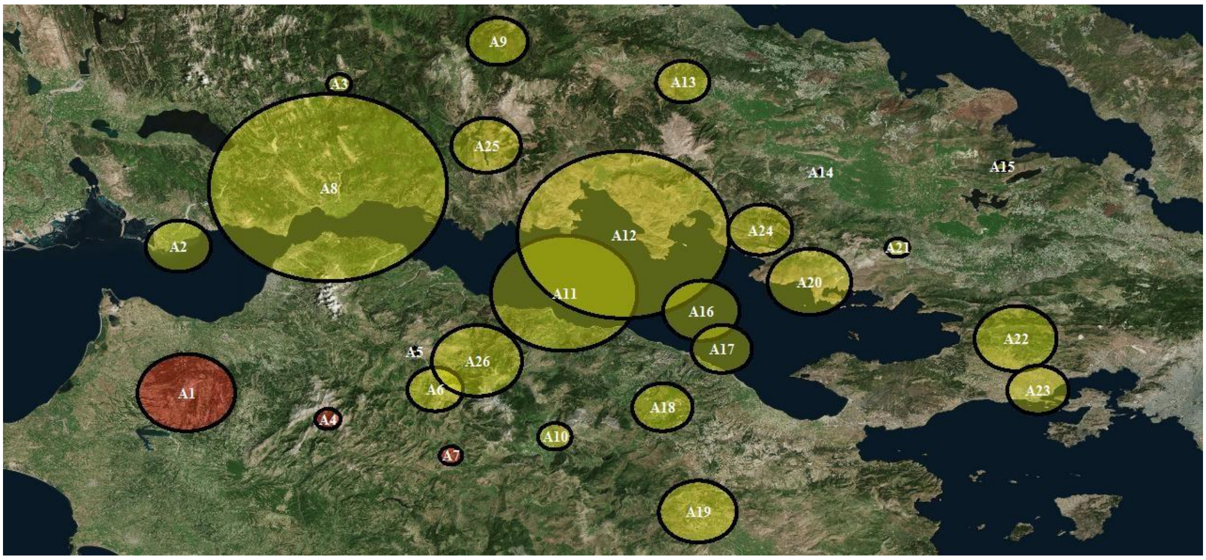

Figure 3. Area strain rate of the study area (yellow ellipses: dilatation, red ellipses: contraction)

Regarding the rotation of the examined area, a dominant clockwise rotation is observed, while the minority (approximately 15%) of the centroids presents counter-clockwise rotation. Rotation values were modelled (-10, -5, -1, 1, 5 and 10 Myr rotation models) in order to be estimated the rotation rates.

Ground deformation modelling, caused by the recent earthquakes of Ionian Islands, Greece

ILIAS LAZOS[1], ALEXANDROS CHATZIPETROS[1], SPYRIDON PAVLIDES[1], STYLIANOS BITHARIS[2], CHRISTOS PIKRIDAS[2], SOTIRIOS SBORAS[3]

[1]*Aristotle University of Thessaloniki, School of Geology, Department of Geology*
[2]*Aristotle University of Thessaloniki, School of Rural and Surveying Engineering, Department of Geodesy and Surveying*
University Campus 541 24, Thessaloniki, Greece
[3]*National Observatory of Athens, Institute of Geodynamics*
Lofos Nymfon, Athens
ilialazo@geo.auth.gr, ac@geo.auth.gr, pavlides@geo.auth.gr, smpithar@topo.auth.gr, cpik@topo.auth.gr, ssboras@gmail.com

Keywords: *seismogenic faults, ground deformation, active tectonics, GPS stations, Ionian Islands*

Abstract

The recent seismic activity of Ionian Sea, Greece, includes two main earthquakes. A seismic event (M_w = 6.1) occurred on January 26th, 2014, in Cephalonia Island, while the main recorded aftershock event was M_w = 5.3. A few days later (on February 3rd, 2014), a second seismic event (M_w = 6.0) occurred, close to the first event area, related to a different fault. Regarding Lefkada Island, a strong seismic event (M_w = 6.4) was recorded on November 17th, 2015. The seismogenic faults led to extended ground deformation, which have been modelled, while the available GPS series have been analyzed.

The Cephalonia seismogenic fault, related to the first event (M_w = 6.1), is a dextral strike slip fault, dipping to the ESE with a high angle. The geometrical characteristics of the fault receive the following values: strike = 23°, dip angle = 68°, rake plunge = 175°. Furthermore, the fault width is 10.0 km, while the top of the fault is located at 7.0 km depth and the bottom of the fault at 16.28 km, based on the aftershock distribution. Concerning the Lefkada seismogenic fault (event of M_w = 6.4), it is considered as the NNE extension of the Cephalonia transfer fault, while it is also dextral. The values of strike, dip and rake are 203°, 88° and 159°, respectively. Based on the aftershock distribution, the estimated fault width is 9.0 km, while the depth of the fault top and bottom is 3.0 and 13.0 km, respectively.

Based on the geometrical characteristics of the seismogenic faults, the horizontal and vertical ground deformation was modelled. In particular, the Cephalonia seismogenic fault presents low horizontal displacement values (1.5 cm) at 0.00 km depth, increasing gradually (4.7 cm) at the fault top (7.00 km depth), receiving the greatest values (8.2 cm) in the middle of the fault (11.64 km depth) and finally decreasing (5.2 cm) at the fault bottom (16.28 km depth). Regarding the vertical displacement, the maximum value difference of the four aforementioned depths is 5.6 mm. The case of the Lefkada seismogenic fault presents remarkably high values (8.7 cm) of horizontal displacement at 0.00 km depth, increasing gradually (11.1 cm) at the fault top (3.00 km depth). At 8.00 km depth (middle of the seismogenic fault), the horizontal displacement receives the highest values (12.6 cm), while at the fault bottom (13.00 km depth) a value decrease is recorded (9.3 cm). The maximum estimated vertical displacement is 18 mm.

The results of modelled and observed ground deformation of the Cephalonia earthquake are similar, as the difference for the horizontal and vertical displacement is 2.5 and 0.2 cm, respectively, based on the permanently installed GPS station (VLSM). Regarding the Lefkada earthquake, the difference between the modelled and observed horizontal displacement is 40.8 and 7.9 cm, respectively, for the two nearest GPS sites (PONT, SPAN). The differences of the vertical displacement are 2.5 cm and 0.4 cm for the same GPS stations. The remarkable difference of the PONT station results is considered that is caused by local displacements, thus were not confirmed by the model implementation.

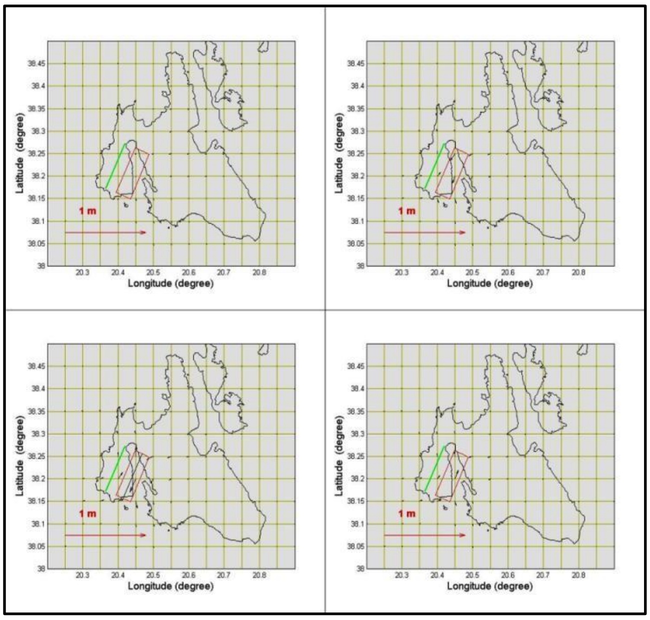

Figure 1. Modelled ground deformation of Cephalonia Island at 0.00 km (top left), 7.00 km (top right), 11.64 km depth (bottom left) and 16.28 km depth (bottom right)

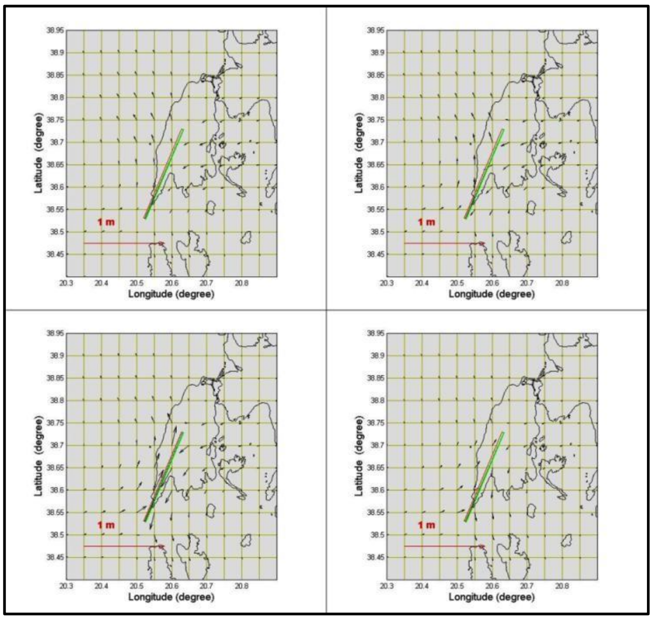

Figure 2. Modelled ground deformation of Lefkada Island at 0.00 km (top left), 3.00 km (top right), 8.00 km depth (bottom left) and 13.00 km depth (bottom right)

Table 1. Total displacement of 3 GNSS stations, due to Cephalonia and Lefkada earthquakes, using GNSS data analysis and Okada model (E-N-U and E'-N'-U', respectively)

Station	Location	Longitude	Latitude	dE (m)	dE' (m)	dN (m)	dN' (m)	dU (m)	dU' (m)
PONT	Lefkada	20.585	38.619	-0.21	-0.01	-0.38	-0.02	-0.06	-0.03
SPAN	Lefkada	20.674	38.781	-0.07	-0.02	-0.06	0.00	0.00	0.00
VLSM	Cephalonia	20.589	38.177	-0.03	-0.01	-0.01	0.00	0.00	0.00

The 2008 (June 8, Mw=6.4) Northwestern Peloponnese (Greece) earthquake: macroseismic intensity assessment using the ESI 2007 and EMS-98 scales and correlation to neotectonic structures and active faults

SPYRIDON MAVROULIS, EMMANUEL SKOURTSOS, GEORGIOS DANAMOS, EFTHYMIOS LEKKAS

National and Kapodistrian University of Athens, School of Sciences, Faculty of Geology and Geoenvironment, Department of Dynamic Tectonic Applied Geology
Panepistimiopolis, 15784, Athens, Greece
smavroulis@geol.uoa.gr, elekkas@geol.uoa.gr

Keywords: *Active faults, earthquake environmental effects, ESI 2007 scale, EMS-98, strike-slip earthquakes*

Abstract

On June 8, 2008, a strike-slip earthquake (Mw=6.4) was generated northeast of the Andravida town (Northwestern Peloponnese, western Greece) due to the activation of the previously unknown western Achaia strike-slip fault zone (WAFZ). Extensive structural damage and earthquake environmental effects (EEE) were induced in the NW Peloponnese, offering the opportunity to test and compare the ESI 2007 and the EMS-98 intensity scales in a moderate strike-slip event.

NW Peloponnese is one of the most tectonically and seismically active regions of Greece. The intense tectonic activity from the Miocene to the Holocene resulted from its location on the external part of the present Hellenic orogenic arc and the close proximity to the present day NNW-SSE trending Hellenic subduction zone. Moreover, the diapiric phenomena of Triassic evaporites originated between Tertiary and Quaternary and caused additional localized deformation. The neotectonic structure of the NW Peloponnese is characterized by the occurrence of large grabens or horsts bounded by E-W or NNW-SSE trending visible or concealed fault zones. Crucial role in the development of the post-alpine formations was played by the tectonic activity during the sedimentation phase, which created smaller horsts and grabens within the major neotectonic macrostructures. The major characteristics of the seismicity of the NW Peloponnese are that all major earthquakes occurred at shallow depths (h < 20 km) and had high intensities ranging from VI to IX.

The structural damage and the EEE induced by the 2008 NW Peloponnese earthquake occurred in an area, where the following neotectonic macrostructures occur: (a) the Patras graben, (b) the Pyrgos-Olympia basin and (c) the Erymanthos Mts horst (Figure 1). They are bounded or cut by active fault zones with Pineios, Peiros, Panopoulo and Western Achaia being the most significant ones.

No effects, which are directly linked to the earthquake energy and in particular to the surface expression of the seismogenic source, were observed in the field. There was no primary surface faulting and the surface deformation was smaller compared to the earthquake magnitude. This fact has been attributed to the thick Gavrovo flysch layer that isolated and absorbed the subsurface deformation from the surface. As regards the secondary EEE, they have been recorded in 29 sites and classified in the following four categories: ground cracks (24%), liquefaction phenomena (28%), landslides (35%) and rockfalls (10%), and hydrological anomalies (3%) (Figure 1). The total areal distribution of secondary EEE was about 800 km^2. Based on this total area, the epicentral intensity is VIII-IX$_{ESI\ 2007}$ and closer to IX$_{ESI\ 2007}$ (Figure 1).

The EEE were classified as marginal to extensive. A maximum local VIII$_{ESI\ 2007}$ intensity has been assigned to several sites (Figure 1), where ground cracks up to 20 cm wide and up to hundreds meters long as well as impressive liquefaction phenomena were observed in post-alpine formations. Intensity VII$_{ESI\ 2007}$ was assigned to the Dafni area, where ground cracks were observed. A minimum intensity equal to V$_{ESI\ 2007}$ was observed within the alpine basement as well as in the post-alpine formations respectively, where small volume (<10 m^3) rockfalls and landslides were triggered (Figure 1). An ESI 2007 intensity map was constructed depicting the spatial distribution of the effects and the ESI 2007 isoseismals (Figure 1).

As far as the building damage is concerned, the dominant building types that suffered damage from this earthquake comprised (a) one or two storey stone masonry buildings with load-bearing walls with insufficient or non-existent seismic resistance design and (b) reinforced concrete (R/C) buildings with R/C frame and masonry infill and partition walls. Most of the R/C buildings were built according to the Greek Seismic Code that was implemented in 1959 with subsequent revisions and upgrades. According to the application of the EMS-98 scale, damage to masonry buildings ranged from grade 3 to 5, while damage in most of R/C buildings ranged from grade 1 to 3. It is concluded that the severity and the distribution of the structural damage was controlled by (a) the local geological and soil conditions and (b) the construction type of buildings.

A maximum ESI 2007 intensity VIII-IX was assigned, while the maximum EMS-98 intensity was IX. For all the sites where intensity VIII has been recorded the ESI 2007 and the EMS-98 agree, but for others the ESI 2007 intensities values are lower by one or two degrees than the corresponding EMS-98 ones, as it is clearly concluded from the comparison of the produced isoseismals (Figure 1). An exception to this rule is the Valmi village, where considerable structural damage occurs (IX_{EMS-98}) along with the lack of significant EEE ($V_{ESI\ 2007}$, Figure 1). This variability between the ESI 2007 and the EMS-98 intensity values is predominantly attributed to the vulnerability of old masonry buildings that have been constructed with no seismic resistance design, suffered damage in previous earthquakes and badly or inadequately restored afterwards.

Therefore, it is concluded that the integration of the ESI 2007 scale with the EMS-98 scale and other traditional intensity scales provides a better picture of the earthquake effect on the built and the natural environment. Moreover, correlation of all existing data shows that the geological structure, the active tectonics, and the geotechnical characteristics of the alpine and post-alpine formations along with the construction type of buildings were of decisive importance in the damage and the EEE distribution.

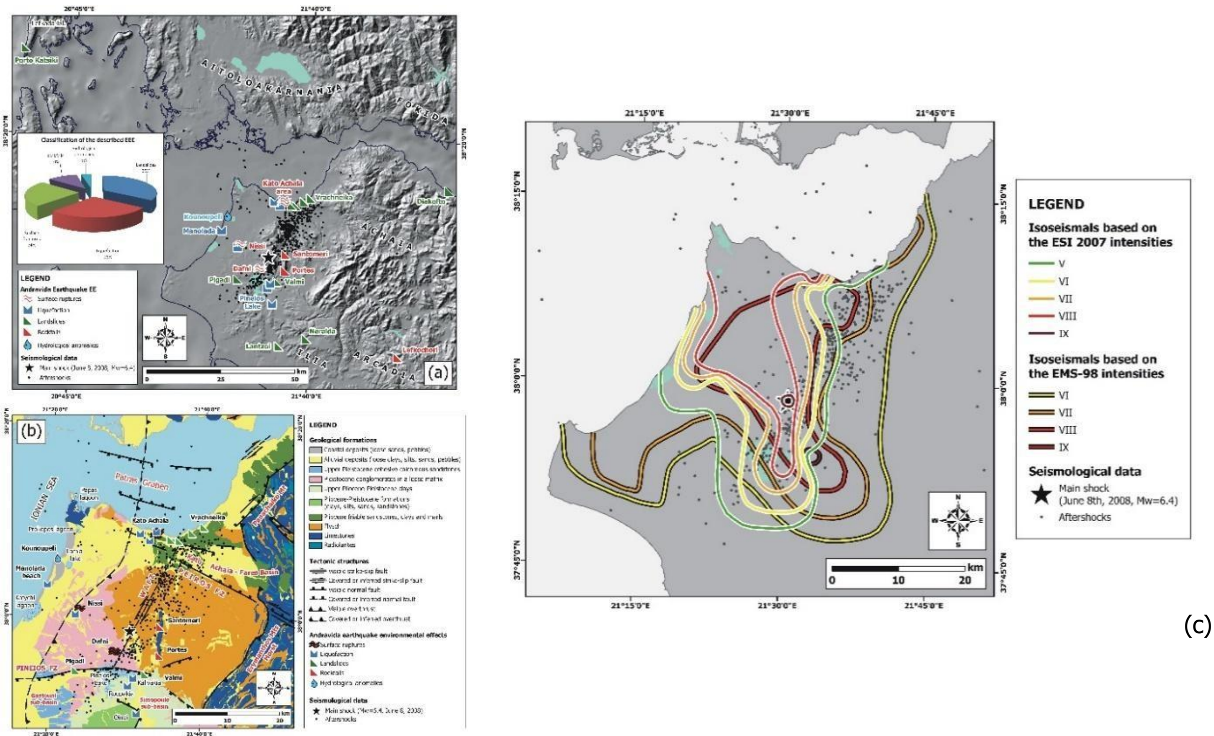

Figure 1. The spatial distribution of the EEE in (a) the NW Peloponnese wide area and (b) in the epicentral area of the 2008 NW Peloponnese earthquake. The percentage distribution of the induced EEE by type is also presented. (c) Comparison, similarities and differences between ESI 2007 and EMS-98 intensities and isoseismals for the 2008 NW Peloponnese earthquake.

Multidisciplinary analysis including neotectonic mapping, morphotectonic indices, applied geophysics and remote sensing techniques for studying recently recognized active faults in Northwestern Peloponnese (Greece)

SPYRIDON MAVROULIS[1], SPYRIDON DILALOS[2], IOANNIS ALEXOPOULOS[2], EMMANUEL VASSILAKIS[3], EFTHYMIOS LEKKAS[1]

[1]*National and Kapodistrian University of Athens, School of Sciences, Faculty of Geology and Geoenvironment, Department of Dynamic Tectonic Applied Geology*
[2]*National and Kapodistrian University of Athens, School of Sciences, Faculty of Geology and Geoenvironment, Department of Geophysics-Geothermics*
[3]*National and Kapodistrian University of Athens, School of Sciences, Faculty of Geology and Geoenvironment, Department of Geography-Climatology*
Panepistimiopolis, 15784, Athens, Greece
smavroulis@geol.uoa.gr, sdilalos@geol.uoa.gr, jalexopoulos@geol.uoa.gr, evasilak@geol.uoa.gr, elekkas@geol.uoa.gr

Keywords: *morphotectonic indices, fault slip rate, photogrammetry, digital shoreline analysis, vertical electrical sounding*

Abstract

A multidisciplinary analysis comprising neotectonic mapping, morphotectonic indices, applied geophysics and remote sensing techniques was applied in the area affected by the 2008 NW Peloponnese (Western Greece) in order to map the recently-recognized E-W striking Pineios River normal fault zone with a high degree of accuracy, and to better understand its contribution to the evolution of the ancient region of Elis during Holocene time.

Quantitative constraints on deformation caused by the faulting were applied through the application of morphometric and morphotectonic indices including drainage network asymmetry, longitudinal river profiles and valley floor slope changes, the river sinuosity index (SI) of modern channels as well as mountain front indices including mountain front sinuosity (Smf) and percentage of faceting along mountain front (F%). All of the aforementioned indicated that the Pineios fault zone is a highly active structure.

The study area consists mainly of a succession of Pliocene to Holocene sediments. Already published $^{230}Th/^{238}U$ dating of corals from the upper layers of the sequence indicates a Tyrrhenian age for samples spanning three complete sections from the footwall of the Pineios fault zone. The deposition ages were determined to be 103 ka for the Psari section (at an elevation of 40-45 m above a.s.l.), 118 ka for the Neapolis section (at an elevation of 60–65 m a.s.l.) and 209 ka for the Aletreika section (at an elevation of140–145 m a.s.l.). The sampling sites that are located north of Pineios fault zone should be located on a single fault block because there is no sign of tectonic disruption between them. The ages of these dated samples correspond to oxygen isotope stages 5.3, 5.5 and 7.3. These stages represent high sea-level stands for the Mediterranean Sea and especially for the western coast of Peloponnese. In particular, at 103 ka sea-level was ~13 m below present sea-level, at 118 ka it was ~1 m below present sea-level and at 209 ka it was ~7 m below present sea-level. From the age of each sample and the sea-level change that has occurred since deposition, uplift rates for the footwall of the Pineios fault zone were calculated as ~0.26 mm/yr for the Psari area, ~0.50 mm/yr for the Neapoli area and ~0.64 mm/yr for the Aletreika area. The maximum uplift rate of 0.64 mm/yr occurs in close proximity to the fault zone. The areas with lower uplift rates are located much further to the north. Because all sample locations are inferred to be within the same fault block, this implies back tilting of the fault block toward north, in full agreement with the rotational block-faulting inferred from structural studies based on field work in the surrounding area.

The rate of uplift for the hanging wall was estimated at ~0.16mm/yr based on a deposition age of 209 ka and a present elevation of 40 m (a.s.l.), which is the lowest elevation that outcrop of Tyrrhenian sediments is found, considering the sea-level change after the deposition. This is much slower even than the slowest measured rate of footwall uplift rate (0.26 mm/yr). The difference between the uplift rate at Aletreika (in the footwall) and the Pineios River plain (in the hangingwall) is ~0.48 mm/yr; this figure corresponds to the slip rate on the Pineios fault zone over the last 209 ka, indicating an overall throw of the fault of ~100 m.

Slip rates were verified by a geophysical survey that measured electrical resistivity along three sections perpendicular to this south-dipping normal fault zone. The geoelectrical data acquisition included 2 "in-situ" resistivity measurements on surface outcrops and 13 Vertical Electrical Soundings. It clearly identifies this tectonic discontinuity at depth where it disrupts depositional layers of different resistivity. Interpretation of the survey results indicates that the fault throw is significantly greater in the westernmost segment of the fault zone, reaching approximately 110 m. This is in good agreement with the fault-slip rate of 0.48 mm/yr that was calculated by the differential uplift rates for blocks on either side of the fault over the past 209 ka.

The continuous activity of Pineios normal fault zone for more than 200 ka has caused relative uplift of the northern block and relative subsidence of the southern block, along with block tilting toward north. The most spectacular landform alteration due to this surface deformation is the N-S migration of the river estuary into completely different open sea areas during the late Quaternary, mainly during the Holocene as well as obvious effects on the shorelines, especially along Kyllini Bay (in the north) where submerged ancient coastlines are known. The sediment transport path has been altered several times due to these changes in river geometry with and the most recent seeming to have occurred almost 200years ago. The river estuary migrated to its contemporary position along the southern coast, settled on the hanging wall, inducing retrograding of the northern coast, and settled on the foot wall, with rates reaching the order of 0.52m/yr, as concluded from historical and recently-acquired remote sensing data. Based on the these data, the rate of retrogradation of this shoreline, which is located on the uplifted fault block, is ~ 0.52 m/yr, due to Pineios River estuary migration since a major source of sediment material transportation, which would have contributed to avoid coastal erosion, has been suspended.

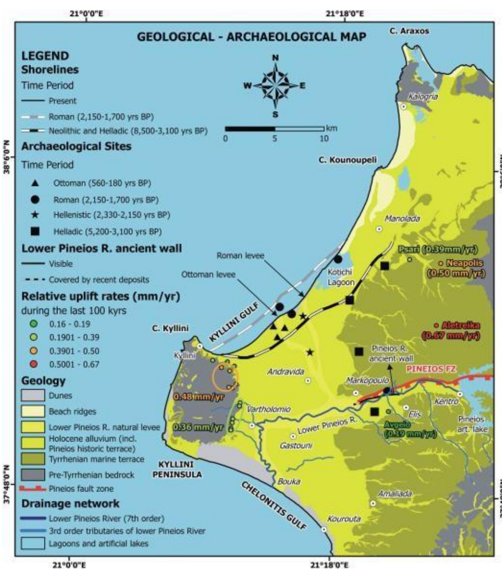

(a)

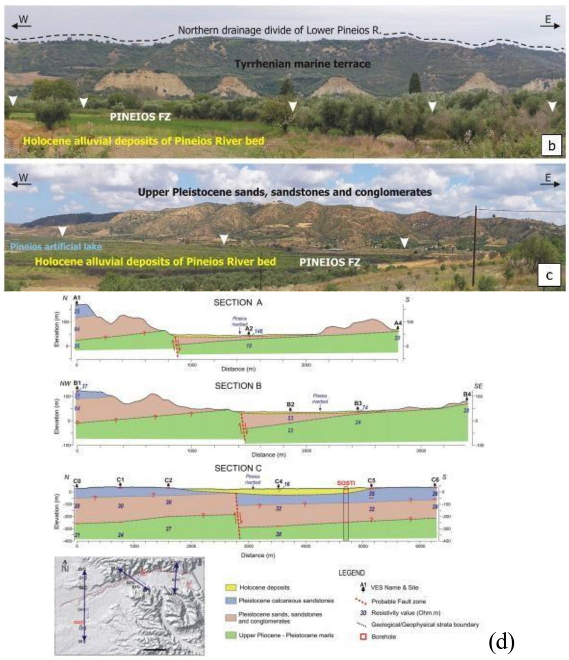

(d)

Figure 1. (a) The geological-archeological map of NW Peloponnese. Partial view of the studied area (b) downstream of the artificial dam, looking toward the Pineios fault zone and (c) upstream of the artificial dam.Well-preserved triangular facets are developed on the Upper Pleistocene deposits. White arrowheads point to the fault trace. (d) Geological sections based on the geophysical data.

The 2016 Mw 7.8 Kaikōura Earthquake: a rare snapshot of coseismic-slip transfer between the plate-interface and faults in the upper-crust

Vasiliki Mouslopoulou[1], Vasso Saltogianni[1], Onno Oncken[1], Andy Nicol[2], John Begg[3], Andrey Babeyko[1], Simone Cesca[1], Marcos Moreno[1]

[1]*Helmholtz Centre Potsdam GFZ German Research Centre for Geosciences*
Potsdam, Germany
[2]*University of Canterbury*
Christchurch, New Zealand
[3]*GNS Science*
Lower Hutt, New Zealand
vasso@gfz-potsdam.de, salto@gfz-potsdam.de, oncken@gfz-potsdam.de, babeyko@gfz-potsdam.de, cesca@gfz-potsdam.de, marcos@gfz-potsdam.de, andy.nicol@canterbury.ac.nz, j.begg@gns.cri.nz

Keywords: *subduction-earthquake, upper-plate, Kaik**ōura**, GPS, marine-biota, uplift*

Abstract

The 2016 M7.8 Kaik**ōura** Earthquake triggered global scientific interest. This is because this earthquake ruptured multiple faults (n>20), mainly onshore, and across an active subduction margin providing, thus, a unique opportunity to examine co-seismic fault interactions between various elements of a subduction system. Although to date, numerous studies have modeled this earthquake, it is still unclear whether or not the plate-interface was involved and if so, to what extent. Here we use published and new field measurements of uplifted marine biota together with displacements recorded by LiDAR, GPS, seismographs and tide-gauges to chart coseismic deformation patterns in the broader Kaik**ōura** region and model the major seismic sources involved in this event. Our analysis captures a rare snapshot of slip-transfer between upper-plate faults and the plate-interface. Despite its apparent involvement in the Kaik**ōura** Earthquake, the plate-interface moved with a mean slip of only 0.4 m. This is because a significant amount of convergent-related slip was accommodated by upper-plate faults that splay off the plate-interface and extends within the upper crust. The Kaik**ōura** earthquake suggests that these large splay-thrust faults may provide a key mechanism in the transfer of plate motion at the termination of a subduction margin and represent an important seismic/tsunami hazard.

The M_w=6.4 2008 Andravida earthquake (Peloponnesus, Greece): ten years after

PANAYOTIS PAPADIMITRIOU, ANDREAS KARAKONSTANTIS, VASILIS KAPETANIDIS, APOSTOLOS AGALOS, ALEXANDRA MOSHOU, GEORGE KAVIRIS, IOANNIS KASSARAS, NIKOLAOS VOULGARIS

Department of Geophysics and Geothermics, University of Athens
Panepistimiopolis, 157 84 Athens Greece
ppapadim@geol.uoa.gr, gkaviris@geol.uoa.gr, kassaras@geol.uoa.gr, voulgaris@geol.uoa.gr

Keywords*: Andravida earthquake, Western Greece, Slip model, Body-wave modeling, relocation of aftershocks*

Abstract

Ten years after the occurrence of the Andravida earthquake (2008) several aspects were investigated, including its connection to neighboring spatiotemporal clusters in the following years. On 8 June 2008 at 12:25 GMT a large earthquake (M_w=6.4) occurred NE of Andravida (Greece) in an area characterized by relatively low seismicity. Nevertheless, it is worth noting that this major event was successfully predicted by a previous study, taking into account decelerating – accelerating seismicity. Data recorded by the Unified Hellenic Seismological Network (HUSN) were analyzed to study the aftershock sequence and local velocity structure. The modeling of teleseismic P, SV and SH waves provided well-constrained focal mechanism solutions of the mainshock and its major aftershocks with magnitude M > 3.4. The constrained fault plane solutions represent dextral strike slip type faulting. The spatial distribution of the aftershocks, as well as the calculation of the slip distribution and Local Earthquake Tomography (LET), provided evidence that the rupture plane is the one with NE-SW direction. Surface breaks were observed in several sites but in most cases their direction was perpendicular to the rupture plane and can be characterized as secondary effects. The source process was characterized by unilateral rupture propagation towards the city of Patras, to the NE, where a seismic sequence was initiated after the M_w=3.9 event of the 27th December 2012 along the ENE-WSW Agia Triada normal fault.

The activation of the pockmark field, in Patras Gulf, triggered by the June 8, 2008 earthquake

GEORGE PAPATHEODOROU[1], DIMITRIS CHRISTODOULOU[1], ELIAS FAKIRIS[1], GIUSEPPE ETIOPE[2], GEORGE FERENTINOS[1]

[1]*Laboratory of Marine Geology and Physical Oceanography, Department of Geology, University of Patras*
Rio, Patras, 26504 Greece.
[2]*National Institute of Geophysics and Volcanology, INGV*
Sezione Roma 2, via V. Murata, 60500143 Roma, Italy
gpapathe@upatras.gr, giuseppe.etiope@ingv.it

***Keywords**: pockmark field, activation, gas plumes, methane, Patras Gulf, earthquake*

Abstract

The Patras Gulf pockmark field consists of 72 pockmarks and extends over an area of about 2.5 km^2 (Fig. 1). The spacing of the individual pockmarks ranges between 20 and 200 m and they are widespread in water depths of 10-45m. The pockmarks are divided into three morphological classes: (i) unit pockmarks measuring from 20 to 40m in diameter and up to 4-5m deep, (ii) normal pockmarks which are mostly circular or oval in plan view, ranging from 50 to 150m in diameter and up to 15m in depth, (iii) complex or composite pockmarks having irregular shape in plan view and occurring as amalgamation of normal pockmarks. Pockmark distribution (pockmark strings) and subbottom profiling data have shown that the pockmark field is fault-controlled.

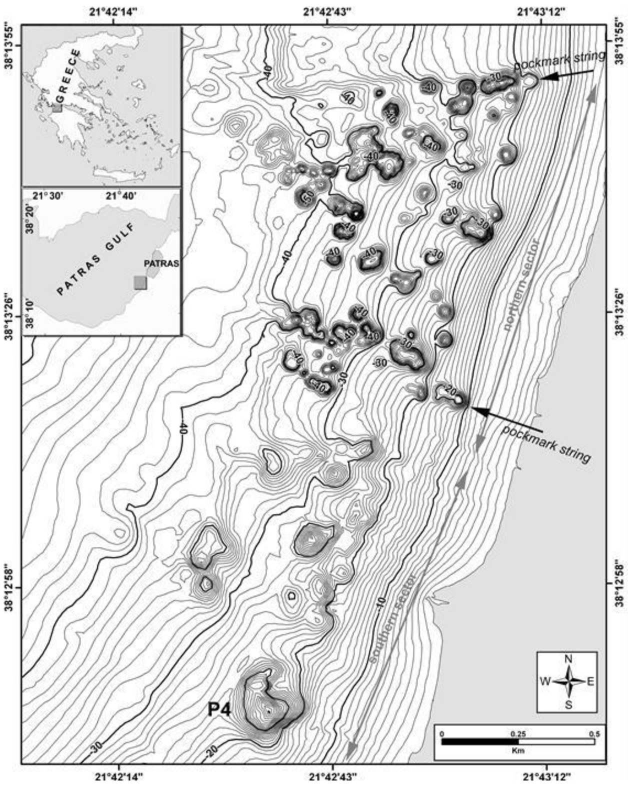

Figure 1. Detailed bathymetric map showing the location of the pockmarks in the Gulf of Patras.

There are strong evidences that the pockmark field activated during a major earthquake of magnitude 5.4 on the Richter scale (July 14th, 1993) (Hasiotis et al., 1996). Judd and Hovland (2007) in his book “Seafloor fluid flow” mentioned that: “*The pockmarks off Patras, northern Peloponnesus, Greece, represent some of the most spectacular and best-documented events in active pockmarks*” (pages 230-231).

On June 8th 2008 (12:25 GMT) a major earthquake, M_W=6.4R, occurred on the Northwestern Peloponnese. Two days after the earthquake and for a period of fifteen days, side scan sonar data and methane measurements were collected in the Patras Gulf pockmark field to find evidence of activation of the field. Gas plumes in the water column above pockmarks recorded on the sonographs (Fig. 2). The number and the volume of the gas plumes were reduced by time. Methane measurements showed high concentrations of dissolved methane in the water column all over the pockmark field.

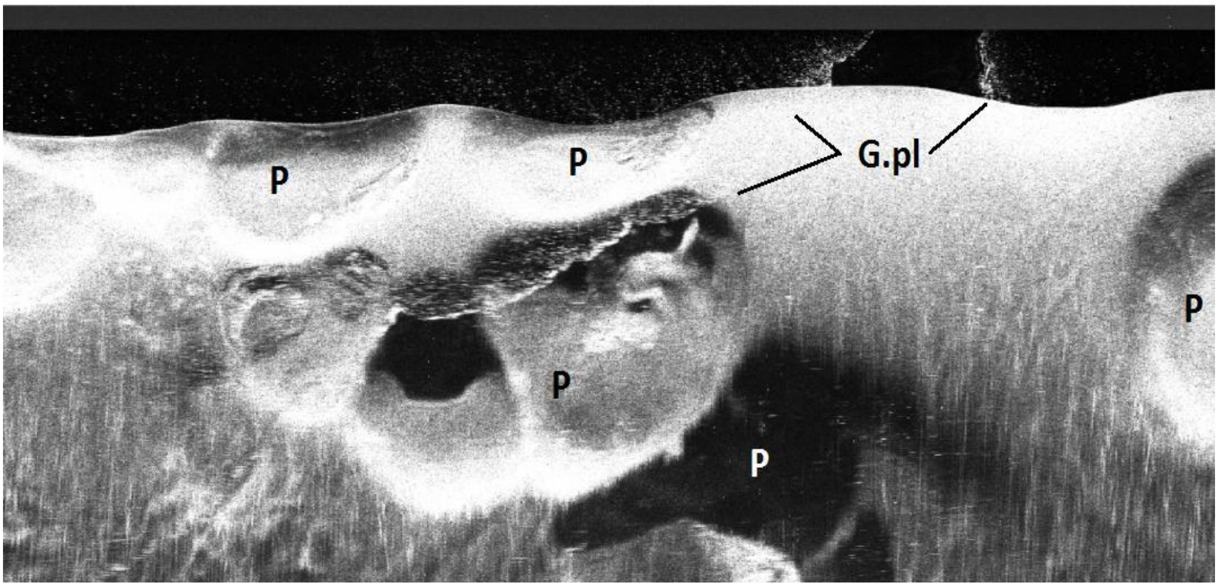

Figure 2. Side scan sonar sonograph taken few days after the 2008 M_W=6.4R Movri Mtn. earthquake showing gas plumes (G.pl) rising from the seafloor of some pockmarks (P).

References

Hasiotis, T., Papatheodorou, G., Kastanos, N., Ferentinos, G. (1996). A pock-mark field in the Patras Gulf (Greece) and its activation during the 14/7/1993 seismic event. Marine Geology, 130, pp. 333-344.

Judd, A. Hovland, M. (2007). Seabed Fluid Flow. The impact on Geology, Biology and the Marine Environment, Cambridge University Press, Cambridge CB2 2RU, UK, p. 475, (www.cambridge.org/9780521819503).

MAΔAM experiment: seismotectonics focus on the Gulf of Patras triple junction

ALEXIS RIGO[1], EFTHIMIOS SOKOS[2], DIMITRIOS GIANNOPOULOS[2], PARIS PARASKEVOPOULOS[2], NIKOS GERMENIS[2], GEORGE ANDRIOPOULOS[2]

[1]*Laboratoire de Géologie, CNRS,ENS, Paris*
24 rue Lhomond 75231 Paris Cedex 5, France
[2]*Seismological Laboratory, University of Patras*
26504 *Rio, Greece*
alexis.rigo@ens.fr, esokos@upatras.gr

Abstract

Although the structure and the dynamics of the Corinth Rift are beginning to be well understood through the efforts done over the past 20 years, its connection with regional tectonic structures remains to be elucidated. The Gulf of Patras appears to be a "triple junction" with the E-W normal faults en echelon of the Corinth Rift to the east, the NW-SE striking Katouna-Stamna fault system (KSF) to the north, the Achaia-Elia strike-slip fault of NE-SW direction to the south where took place the 2008 Movri earthquake, these two fault systems being connected to the Lefkada-Kefalonia fault system, and the southwestern subduction. It was thus proposed to define a block or microplate that Pérouse (2013) and Pérouse et al. (2017) denotes IAB for Islands Arkananian Block. Since the automn of 2015, we maintain a temporary seismological network (MADAM experiment) of 16 stations deployed between the northern coast of the Gulf of Patras and the north of the Gulf of Amvrakikos. The aim of this network is to constrain the deformation of the northwest boundary of the microplate IAB, and its crustal structure. We will present here the very preliminary results of the Madam seismic survey, and the following project we are promoting in order to deploy a seismic network including OBS in the Gulf of Patras extending the study area to the west and to the south.

References

Pérouse, E. (2013). Cinématique et tectonique active de l'Ouest de la Grèce dans le cadre géodynamique de la Méditerranée Centrale et Orientale. Université Orsay - Paris Sud, Paris XI

Pérouse, E., Sébrier, M., Braucher, R., Chamot-Rooke, N., Bourlès, D., Briole, P., Sorel, D., Dimitrov, D., Arsenikos, S. (2017). Transition from collision to subduction in Western Greece: the Katouna–Stamna active fault system and regional kinematics. International Journal of Earth Sciences.

The interplay between active tectonics and sea-level fluctuations and their impact on the evolution of the prehistoric landscapes in the Aegean Region

DIMITRIS SAKELLARIOU, ALEXANDRA ZAVITSANOU, KONSTANTINA TSAMPOURAKI-KRAOUNAKI, GRIGORIS ROUSAKIS

Institute of Oceanography, Hellenic Centre for Marine Research
19013 Anavyssos, Greece
sakell@hcmr.gr

Keywords: *vertical tectonics, transtension, transpression, eustatic changes, relative subsidence/uplift*

Abstract

The Aegean Region, including the Hellenic Arc, is the tectonically most active area in Europe. Recent progress in the understanding of its deformation show that the Aegean crust "flows" toward SSW, confined between the North Anatolian and Kephallinia Faults to the North and Northwest and the East Hellenic Trench to the Southeast. The deformation is accommodated by dextral and sinistral shearing which create a complex pattern of localized transtensional features along with local transpressional deformation and local uplift. Building up of stresses along the boundaries and in the interior of the involved crustal blocks leads to vertical and horizontal movements accommodated by normal, thrust and strike-slip faults.

Long-term, tectonic uplift and/or subsidence throughout the Quaternary is evident at many places along the Hellenic Arc and within the Aegean Region, and has been documented with mapping and dating of uplifted Pleistocene marine terraces or submerged prodelta prograding sequences. Local tectonic processes during the Late Holocene are additional to the modeled post-LGM sea level rise and can amount to 6m or more vertical displacement of palaeo-shorelines up or down. These are observed in numerous places along the Aegean coastline, including Crete, Rhodes, Gulf of Corinth, Evia Island, the Aegean Islands etc. Differential tectonic movements in Central Greece have led to localized subsidence and the creation of deep basins below the Gulf of Corinth, North Evia, West Saronikos Gulf and other gulfs. All of these currently marine basins were isolated lakes during the LGM and their water-level varied from the surrounding sea-level. Submerged historic and prehistoric settlements and sea-level indicators occur close to uplifted marine terraces (or vice versa) and challenge the published sea-level curves which result from the modeling of eustatic and isostatic processes.

Active tectonics in the Aegean is the major driving mechanism which has controlled and defined the development of long-term subsiding, deep basins with continuous sedimentation during Quaternary and has outlined the crustal blocks which have escaped subsidence or exhibit long-term, continuous or episodic, relative uplift. The latter represent the areas which have been exposed during the low sea-level periods and bear the potential of hosting prehistoric landscapes and therefore traces of Paleolithic archaeology. Understanding of the local and regional vertical tectonic movements and history throughout Pleistocene is essential for the definition of the most promising areas to be surveyed for submerged landscapes by means of modern marine survey techniques.

Due to the long-term tectonic activity and the continuously evolving landscape, the geography of the Aegean Region in any given high or low sea-level stage has never persisted into the next stage. The interplay between periodically fluctuating sea level and long-term tectonic activity has led to the formation of extended landmasses during Pleistocene low sea level stages, separated from each other by narrow sea straits. The North Aegean Island Bridge, the Central Aegean Island Bridge, the West and East Cretan Straits and the northern part of the Ionian Margin display this type of paleogeographical configuration and may represent areas where early seafaring has evolved. Opposite land tips on either sides of narrow sea-straits may also be of major importance for prehistoric occupation and migration and thus may host traces of prehistoric human presence.

25-Year Ground Deformation Studies in the broader Area of Patras Gulf based on Geodetic and Radar Interferometric techniques

VASSILIS SAKKAS[1], EVANGELOS LAGIOS[1], MAITE GARCIA[2], MARCO BIANCHI[2]

[1]*Department of Geophysics-Geothermics, National and Kapodistrian University of Athens*
Panepistimiopolis, Ilissia,15784 Greece
[2]*TRE ALTAMIRA SLU*
Còrsega 381-387, 08037 Barcelona, Spain
vsakkas@geol.uoa.gr, lagios@geol.uoa.gr, maite.garcia@tre-altamira.com, marco.bianchi@tre-altamira.com

Keywords: *Ground Deformation, Satellite Geodesy GPS, SqueeSAR Interferometry, Sentinel*

Abstract

The broader area of Patras Gulf is an asymmetric rift being consisted of WNW-ESE trending normal faults of listric shape as a result of the tensional stress regime. The area is characterized by intense seismic activity with a large number of earthquakes of magnitude M>5 occurred in the vicinity of the area during the last 25 years. The focal mechanisms of the last major earthquakes in the vicinity of Patras Gulf have shown a NE-SW trending zone that crosses the area. Several others events have also occurred adjacent to the Patras Gulf and mainly along the Cephalonia Transform Fault and south of Zakynthos Island on the west. A prominent feature of the seismicity distribution is the absence of intense seismic activity in the marine area of Patras Gulf when compared to the broader area. The absence of seismicity may be indicative of the lack of major faulting systems in the area, or active faults in the area. However, it has to be noticed that the submarine area has not been fully mapped, yet. A ten-station GPS network extending in the broader area of Patras Gulf was established in 1994 to study the local and regional ground deformation of the area. Together with the campaign geodetic measurements daily processing was executed to Continuous GPS data (cGPS) from several stations established in the area since 2006. On a regional scale, horizontal and vertical motion was estimated with respect to IGb08 using data also from the continuous GPS (cGPS) stations. A ground deformation having direction of ESE to SE was observed with a rate of ~10 - 20 mm/yr across the gulf. The southern part exhibited a more SE oriented displacement, while the northern part had an eastward orientation. Concerning the vertical velocity component small velocity values were observed ranging from -2 to +1 mm/yr. The horizontal deformation vectors revealed an extension of the Patras Gulf: The southern part seems to be extending to SE with amplitudes of 8 - 13 mm/yr, while in the northern part, a differentiation of the motion exists between its westernmost and eastern segment.

Interferometric processing of SENTINEL 1A radar data, using the SqueeSAR™ technique covering the period October 2014 to February 2015 for both ascending and descending orbital geometries. The interferometric products were jointly interpreted with the non-EO data (geological, tectonic, seismological and geodetic) at an effort towards the identification and verification of known and "hidden" active faulting zones that consecutively facilitated the better assessment of the Seismic Hazard characterization for this area. 78 and 68 SENTINEL1A (S1A) radar images of ascending and descending orbital geometry, respectively, were processed for the observational period October 2014 to February 2017. About 200,000 PS/DS points were identified in the final products, with a coherence threshold of 0.7. The *ascending* and *descending* data were further processed in order to extract *Acceleration* maps of the area as well as they were decomposed in *East-West* and *Vertical* motion maps.

The overall image of both ascending and descending orbital geometries (Fig. 1) shows small LOS velocity values ranging from -4 to +4 mm/yr. Increased values of mostly negative LOS velocities (<-8 mm/yr) are observed mainly along some major faulting zones that were active during this time period (e.g. the Psathopyrgos zone, NE of Patras) or in areas where subsiding and landsliding phenomena may occur (mountainous slopes south of Patras). From both geometries it is evident that differential motions are identified along the main faulting features of the area, but also in areas where no major faulting zone exist. Comparing the ascending and descending orbital geometries, a qualitative

interpretation of the *vertical* and *East-West* components may also be deduced. Negative LOS velocities indicate subsidence and/or eastward horizontal motion for ascending geometry, while in descending geometry the horizontal component has a westward direction. Based on these remarks vertical motions (mainly subsidence) observed in the urban environment of Patras City, as well as on the down-throw side of Psathopyrgos Fault. Small negative LOS velocity values on ascending geometry and positive values on descending geometry south and west of Patras City may be considered as indicative of an eastward horizontal motion in the area.

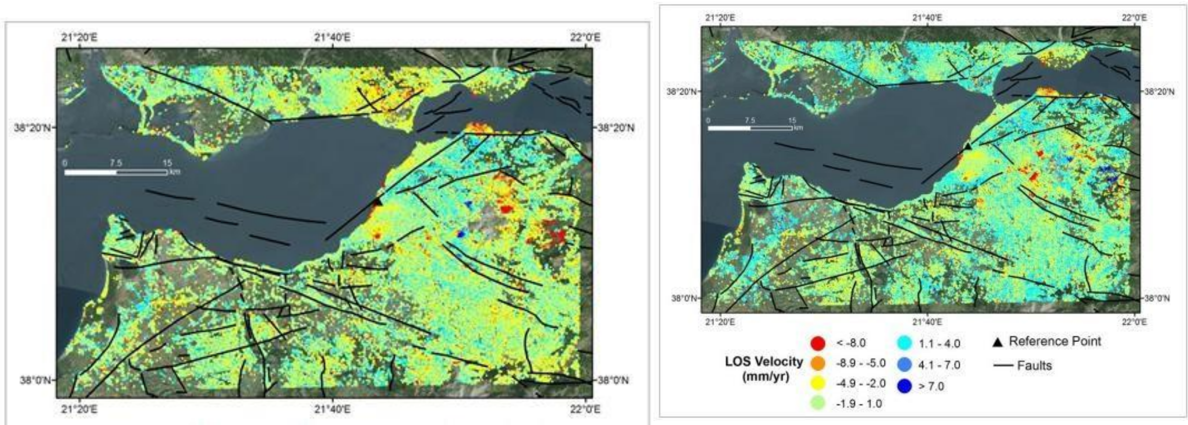

Figure 1. LOS velocity field form SqueeSAR^{TM} interferometric analysis on Ascending (left) and Descending (right map) orbital geometries in Patras Gulf.

The purpose of all the applied methodologies was for the better understanding of the tectonic regime, and assesses the potential of a strong earthquake close to the urban center of Patras. The joint interpretation of the available non-EO data with the interferometric results and the extracted products (acceleration and motion components) provide the necessary "input" in order to better assess the seismic hazard characterization. The spatial coverage of the interferometric data provided new understanding of how the surface is being deformed with respect to the main tectonic features, as well as due to other reasons (e.g. subsidence due to water extraction). Important evidence of active faults was retrieved based on the interferometric results.

Many active faults and zones are known in the broader area of Patras Gulf that have the potential to generate strong earthquakes. The most active one is the Psathopyrgos Fault to the NE of Patras and its possible continuation to the west that almost cross-cuts the City of Patras. This faulting system has generated many intermediate earthquakes in the recent past ($3.0<M<4.2$) and is considered capable of generating earthquakes of ~M6. The seismic activity seems to show a periodic migration towards the West (and to Patras City), and then shifts back to the East. The LOS velocity field on both orbital geometries has clearly depicted the differential motion along this fault with a small rate (~4mm/yr^2), but with a significant velocity (~8mm/yr). The strong differential deformation becomes more evident when inspecting the vertical component, which deduced by decomposing Ascending and Descending data, that shows subsidence of ~5mm/yr. The almost linear type of motion, revealed by both geodetic and interferometric data,combined with the continuous small seismic activity occurring in the area, may indicate a gradual release of the seismic energy. However, stress may be accumulated as a result of the differential stress field in between Corinth Gulf (on the East) and Patras Gulf (on the West) that may be discharged along one of the main tectonic zones cross-cutting the entire region of Patras Gulf.

New Constraints from Seismology and Geodesy on the Mw=6.4 2008 Movri (Greece) Earthquake

ANNA SERPETSIDAKI[1], PANAGIOTIS ELIAS[2,3], MAYA ILIEVA[2,4], PASCAL BERNARD[5], PIERRE BRIOLE[2], ANNE DESCHAMPS[6], SOPHIE LAMBOTTE[7], HELENE LYON-CAEN[2], EFTHIMIOS SOKOS[1], G-AKIS TSELENTIS[3].

[1]*Seismological Laboratory, University of Patras*
Patras, Greece
[2]*Laboratoire de Géologie, Ecole Normale Supérieure, CNRS*
Paris, France
[3]*National Observatory of Athens*
Athens, Greece
[4]*Bulgarian Academy of Sciences*
Sofia, Bulgaria
[5]*Institut de Physique du Globe de Paris, CNRS*
Paris, France
[6]*GéoAzur, Université de Nice Sophia Antipolis - CNRS - IRD – OCA*
France
[7]*Ecole et Observatoire des Sciences de la Terre, CNRS*
Strasbourg, France
annaserp@upatras.gr, pelias@noa.gr, ilieva@mailhost.geologie.ens.fr, bernard@ipgp.jussieu.fr, pierre.briole@ens.fr, deschamps@geoazur.unice.fr, sophie.lambotte@unistra.fr, helene.lyon-caen@ens.fr, esokos@upatras.gr

Keywords: *Earthquake dynamics, Seismicity and tectonics, Dynamics and mechanics of faulting*

Abstract

The 2008 M_w=6.4 Movri earthquake ruptured a NNE right lateral strike slip fault about 30 km south of the city of Patras. Although some strike slip activity on minor faults was known, there was no tectonic evidence of large scale NS striking fault and such a large event was not anticipated. Following the event, a network of six stations was installed for four months in the epicentral area in order to monitor aftershocks and in particular the northern part of the rupture area closest to the city of Patras. We combine these new aftershock observations with GPS measurements of an already existing geodetic network in the area performed just after the earthquake, together with already published source studies, in order to refine already proposed models of this event. The combined data set allows defining much more accurately the lateral and vertical limits of the rupture. Its length inferred from geodesy is ~15 km and its modelled upper edge ~17 km. The seismic moment then constrains the lower edge to coincide, within a few kilometres, with the Moho interface. The absence of seismicity in the shallow crust above the co-seismic fault is interpreted as a result of the decoupling effect of possible presence of salt layers above the rupture area, near 14 to 16 km in depth, which favors our interpretation of an immature strike slip fault system, compatible with the absence of surface ruptures. The immature character of this large crustal fault is further suggested by the high variability of focal mechanisms and of fault geometries deduced from aftershock clusters, in the strike direction. Its geometry and mechanism is consistent with the crustal shear, striking NNE, revealed by GPS in this region. This shear and faulting activity might be generated by the differential slip rate on the subduction interface, 50 km to the south, leading to a north-northeastward propagating strike-slip fault zone. The wide extension of the aftershock distribution forming a NNE alignment, beyond the rupture area towards the north, suggests a localization process of the shear strain, which could be the preliminary stage of fault propagation further to the NNE. An alternative speculative model for this regional stress could be the existence of a well developed NNE striking shear zone within the uppermost mantle, marking at depth the southward propagation of the northern branch of the North Anatolian fault. Both models may not be exclusive of each other, and in fact their sources may be mechanically interdependent.

From the behavior of fault gouges to earthquake nucleation and control

IOANNIS STEFANOU

Laboratoire Navier, UMR 8205, Ecole des Ponts, IFSTTAR, CNRS, UPE
Champs – sur – Marne France
ioannis.stefanou@enpc.fr

Abstract

The thermo-hydro-chemo-mechanical (THMC) behavior of fault gouges is central for earthquake nucleation in mature faults. In this talk we revise the basic mechanisms leading to the transition from aseismic to seismic slip (dynamic instability) focusing mainly on the role of:

a) the full stress-strain response of the fault gouge,

b) the thickness of the Principal Slip Zone and of the size of the evolving microstructure and

c) the apparent rate dependency of the system due to THMC couplings (thermal pressurization).

The analysis is based on theoretical and numerical considerations. Comparisons with in-situ observations show a good agreement with the theoretical findings regarding qualitative behavior of the system and the thickness of the principal slip zone. Shedding light upon the detailed response of fault gouges is a cornerstone in induced seismicity and earthquake control.

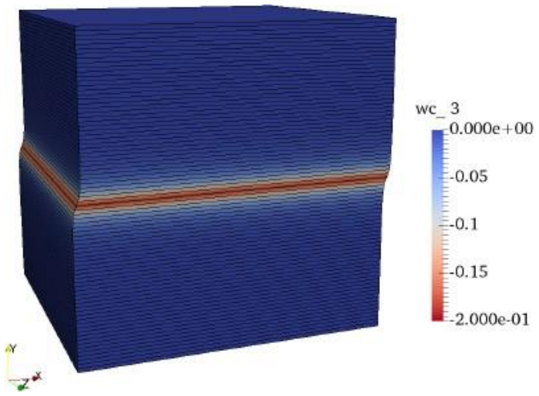

Figure 1. Development of the Principal Slip Zone inside a fault gouge (red indicates increased shear intensity).

References

Rattez, H., Stefanou, I., Sulem, J. (2018). The importance of Thermo-Hydro-Mechanical couplings and microstructure to strain localization in 3D continua with application to seismic faults. Part I: Theory and linear stability analysis. Journal of the Mechanics and Physics of Solids, 115, 54-76.

Rattez, H., Stefanou, I., Sulem, J., Veveakis, M., Poulet, T. (2018). The importance of Thermo-Hydro-Mechanical couplings and microstructure to strain localization in 3D continua with application to seismic faults. Part II: Numerical implementation and post-bifurcation analysis. Journal of the Mechanics and Physics of Solids, 115, 1–29.

Stefanou, I., Sulem, J. (2014). Chemically induced compaction bands: Triggering conditions and band thickness. Journal of Geophysical Research: Solid Earth, 119(2), 880–899.

Kinematic compatibility and paleostress analysis of heterogeneous fault-slip data from Kopaonik Mts. (Southern Serbia)

MARKOS TRANOS, GEORGE GEORGIADIS

Department of Geology, Aristotle University of Thessaloniki
54124 Thessaloniki, Greece
tranos@geo.auth.gr, gggk@geo.auth.gr

Keywords:*fault-slip analysis, stress inversion, heterogeneous fault-slip data, Dinarides, Serbia.*

Abstract

The late- and post-collisional deformation in an orogen is not a simple issue and much more difficult to decipher since it may involve several stages and the obliteration or reactivation of previous structures by newer events. The interest in this deformation is increased when it is associated with magmatism, basin formation and exhumation processes as is the case of the area in the boundary between the Dinarides and the Carpatho-Balkan orogen. Considering these, similar fault-slip data with those published by Mladenović et al. (2015) for the area of Kopaonik Mts. (southern Serbia) are used, in order to investigate the efficiency of different fault-slip analyses and stress inversion methods indefining correctly the paleostress tensors and to unravel the paleostress history of a region. The study area in the west comprises rocks that belong to the innermost thrust sheets of the Dinarides, the Drina-Ivanjica and the Jadar-Kopaonik-Studenica, the Western Vardar Ophiolitic Unit, and in the east rocks belonging to the Eastern Vardar Ophiolitic Unit that is part of the Carpatho-Balkan orogen. Several bodies of extrusive and intrusive rocks, dated in Oligocene – Miocene, are found to cut or cover the previously mentioned rocks (Mladenović et al. 2015).

A total of 496, contractional and extensional, fault-slip data from 13 different stations were used. In contrast with Mladenović et al. (2015) who separated them manually and calculated paleostress tensors at each station, we consider all of them as a single fault-slip data set without using tectono stratigraphic criteria. The fault-slip data are heterogeneous and because of this, following the approach of Tranos & Lacombe (2014), they are separated in homogeneous groups (PT groups) using their kinematic axes (P and T axes) in order to calculate the regional stress tensors. An additional restriction laid down in this approach is that each group should include fault-slip data from more than one station, so that the fault slips are not a result of local stresses. A total of 17 groups, including 297 fault-slip data, were used for further analysis and a stress tensor was calculated for each of these groups. These stress tensors were compared and merged taking into account (a) the vertical axis, (b) the stress ratio and (c) the trend of the horizontal axis. The six stress tensors (TB1-TB6) that resulted from these procedure, were applied to the total population of the 496 fault-slip data in order to define which additional fault-slip data and thus the PT group they belong, can be driven by these stress tensors using a 30° misfit angle (MA) criterion (the same MA criterion used by Mladenović et al. 2015). The fault-slip data of those PT groups that were not used in the analysis so far and were dynamically compatible with one of the calculated stress tensors were added to the TB1-TB6 fault-slip data, respectively, resulting in six enhanced stress tensors TC1-TC6. TC1 is a pure compressional (PC) stress tensor with a NNW-SSE trending maximum stress axis (σ_1). TC2 defines a strike-slip – transpressional (SS-TRP) stress regime with a NE-SW trending σ_1 and a NW-SE trending σ_3. TC3 defines a strike-slip – transtensional stress (SS-TRN) regime with a NW-SE trending σ_1 and a NE-SW trending σ_3. TC4 is a pure extensional – transtensional (PE-TRN) stress tensor with a NNW-SSE trending minimum stress axis (σ_3). TC5 defines a pure extensional (PE) stress regime with a NNW-SSE trending σ_3, and finally, TC6 defines a radial extension - pure extension (PE-RE) with a WNW-ESE trending σ_3. In order to examine the stress difference between these stress tensors, and thus the robustness of the solution, the stress tensors were compared using the Stress Tensor Discriminator Faults (STDFs) (Tranos, 2015, 2017, 2018) as the latter result from application of these stress tensors to the whole 496 fault-slip dataset. This examination showed that all the calculated stress tensors were different from each other,

except from TC4 and TC5 that could not be differentiated sufficiently.
The results of the above mentioned analysis were compared with the results of Mladenović et al. (2015) and also with the results of Kounov et al. (2011) and Tranos & Lacombe (2014), which carried out paleostress analyses in nearby areas also close to the boundary of the Dinarides with the Carpatho-Balkan orogen. The comparison shows that the paleostress analysis of a multi-deformed region is possible even in the absence of tectonostratigraphic criteria, but the paleostress tensors strongly depend on the adapted process used for the separation of the recorded fault-slip data into homogeneous groups. Another conclusion is that the paleostress analysis of a multi-deformed region into which the recorded fault-slip data are heterogeneous is at least more comprehensive when the stress inversion process is applied not only to stations, but to the whole volume of rock, because in this way the stress tensors are calculated from fault-slip data with widespread orientations and represent the deformation of the whole area and not a possible local differentiation of the stress field. An interesting issue is that even if similar paleostress tensors have been defined, their interpretations and dating might differ amongst the researchers depending on the geological-tectonic context they adopted.

References

Kounov, A., Burg, J.-P., Bernoulli, D., Seward, D., Ivanov, Z., Dimov, D. Gerdjikov, I. (2011). Paleostress analysis of Cenozoic faulting in the Kraishte area, SW Bulgaria. J. Struct. Geol., 33, 859-874.

Mladenović, A.,Trivić, B. Cvetković, V. (2015). How tectonics controlled post-collisional magmatism withing the Dinarides: inferences based on study of tectono-magmatic events in the Kopaonic Mts. (Southern Serbia). Tectonophysics, 646, 36-49.

Tranos, M.D. (2015). TR method (TRM): A separation and stress inversion method for heterogeneous fault-slip data driven by Andersonian extensional and compressional stress regimes. J. Struct. Geol., 79, 57–74, doi: 10.1016/j.jsg.2015.07.006.

Tranos, M.D. (2017). The use of Stress Tensor Discriminator Faults in separating heterogeneous fault-slip data with best-fit stress inversion methods. J. Struct. Geol., 102, 168-178, doi:10.1016/j.jsg.2017.08.002.

Tranos, M.D. (2018). The use of Stress Tensor Discriminator Faults in separating heterogeneous fault-slip data with best-fit stress inversion methods. II. Compressional stress regimes. J. Struct. Geol., 107, 153-162, doi: 10.1016/j.jsg.2017.12.015.

Tranos, M., Lacombe, O. (2014). Late Cenozoic faulting in SW Bulgaria: Fault geometry, kinematics and driving stress regimes. Implications for late orogenic processes in the Hellenic hinterland. Journal of Geodynamics, 74, 32-55, doi:10.1016/j.jog.2013.12.001.

The lethal earthquake of 15th July 1909 in Chavari, Elis: a little known event

IOANNA TRIANTAFYLLOU[1,3], IOANNIS KOUKOUVELAS[2], GERASSIMOS PAPADOPOULOS[1]

[1]*Institute of Geodynamics, National Observatory of Athens*
Athens 11810, Greece
[2]*Department of Geology, University of Patras*
Patras 26500, Greece
[3]*Department of Dynamic, Tectonic and Applied Geology, Faculty of Geology and Geoenvironment, National & Kapodistrian University of Athens*
Athens, 15784, Greece
ioannatriantafyllou@yahoo.gr, iannis@upatras.gr, papadop@noa.gr

Keywords: *Chavari, NW Peloponnese, moderate earthquake, high intensity, buildings collapse, human victims, precursors, ground failures*

Abstract

On 15th July 1909 (NS) a moderate earthquake of M~5.7 occurred in Chavari village close to Ancient Elis, NW Peloponnese. It was reported that the earthquake was lethal but no details were provided (e.g. reports of National Observatory of Athens, NOA, 1909). The earthquake has been listed in some earthquake catalogues but is ignored in others. From newspaper information an attempt was made recently to reconstruct the intensity field of the earthquake (Misailidis et al., 2014). However, this earthquake event remains very little known up to now since the collected information about its effects has been quite limited. To study further this event we collected a wealth of information from primary and secondary sources. The primary sources include the unpublished „Book of Earthquakes“ of the Institute of Geodynamics of NOA as well as an exhaustive compilation of local, national and international press reports. The secondary sources include various earthquake catalogues and other scientific publications as well as local books including photos illustrating the disastrous effects of the earthquake. From the examination and the cross-checking of the sources we found that the earthquake event, although of moderate magnitude, has been highly lethal causing a death toll of 55 and 284 injuries mainly in Chavari but also in the surrounding villages. Maximum intensity of IX-X was estimated in Chavari. A variety of earthquake associated phenomena were also reported, including ground failures (e.g. extensive soil liquefaction in several spots) and hydrological changes. In addition, precursory phenomena were observed, such as anomalous animal behavior and earthquake lights. From the collected descriptions we tentatively suggest that the seismic fault ruptured very close to Chavari and was of normal type. However, a field campaing is needed for the investigation of possible surface fault trace.

INDEX

2nd Scientific Meeting of the Tectonics Committee of the Geological Society of Greece

10 Years after the 2008 Movri Mtn M6.5 Earthquake;
An earthquake increasing our knowledge for the deformation in a foreland area

<u>Invited Speaker : Riccardo Caputo, Ferrara University (Italy)</u>

VENUE: Conference & Cultural Center of the University of Patras
Patras, 13 June 2018

Organizers

Sponsor

2^{nd} Scientific Meeting of the Tectonics Committee of the Geological Society of Greece

10 Years after the 2008 Movri Mtn M6.5 Earthquake; An earthquake increasing our knowledge for the deformation in a foreland area

PROGRAMME

Sponsor

Patras, Greece
13 June 2018
Conference and Cultural Center of the University of Patras

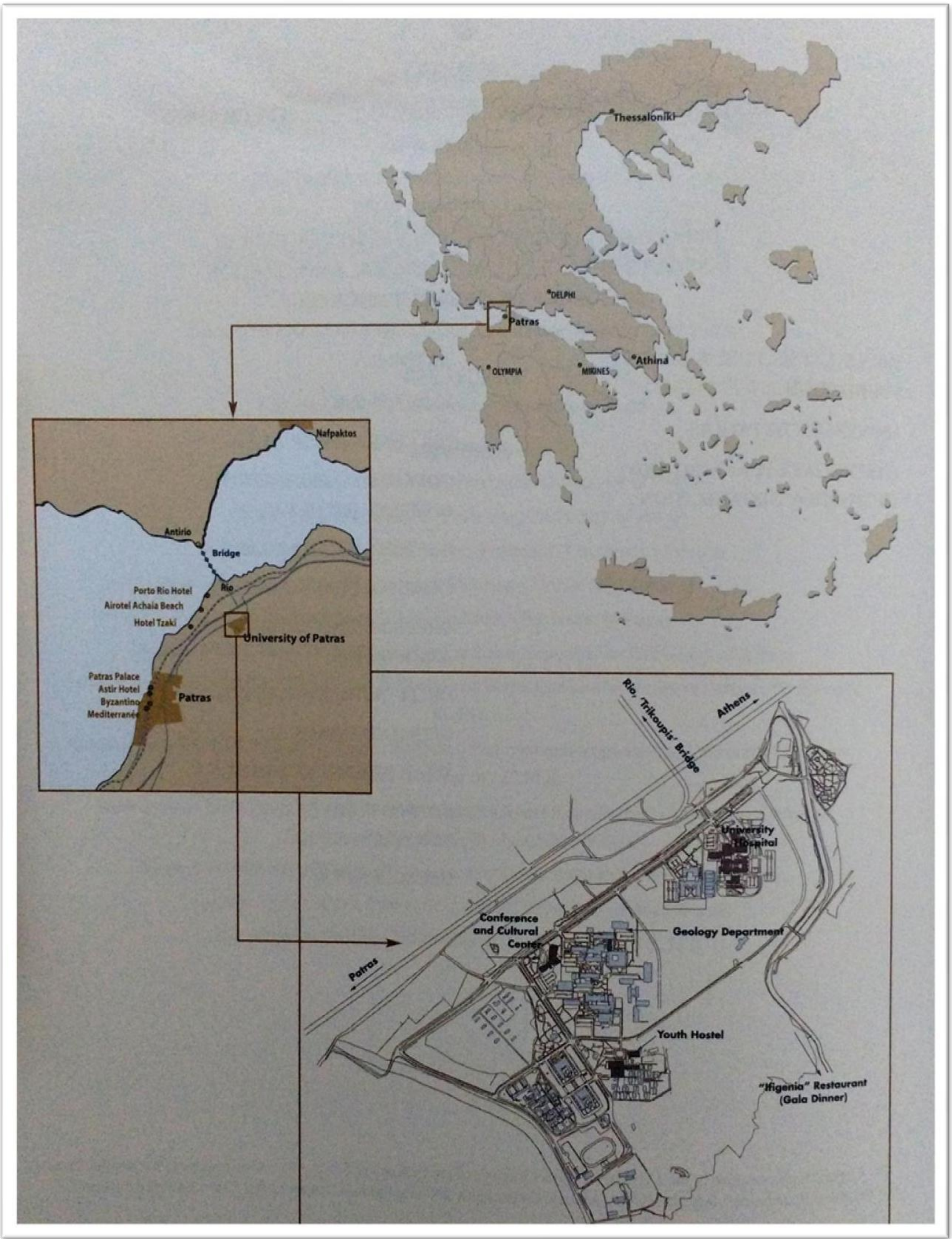

Location Map

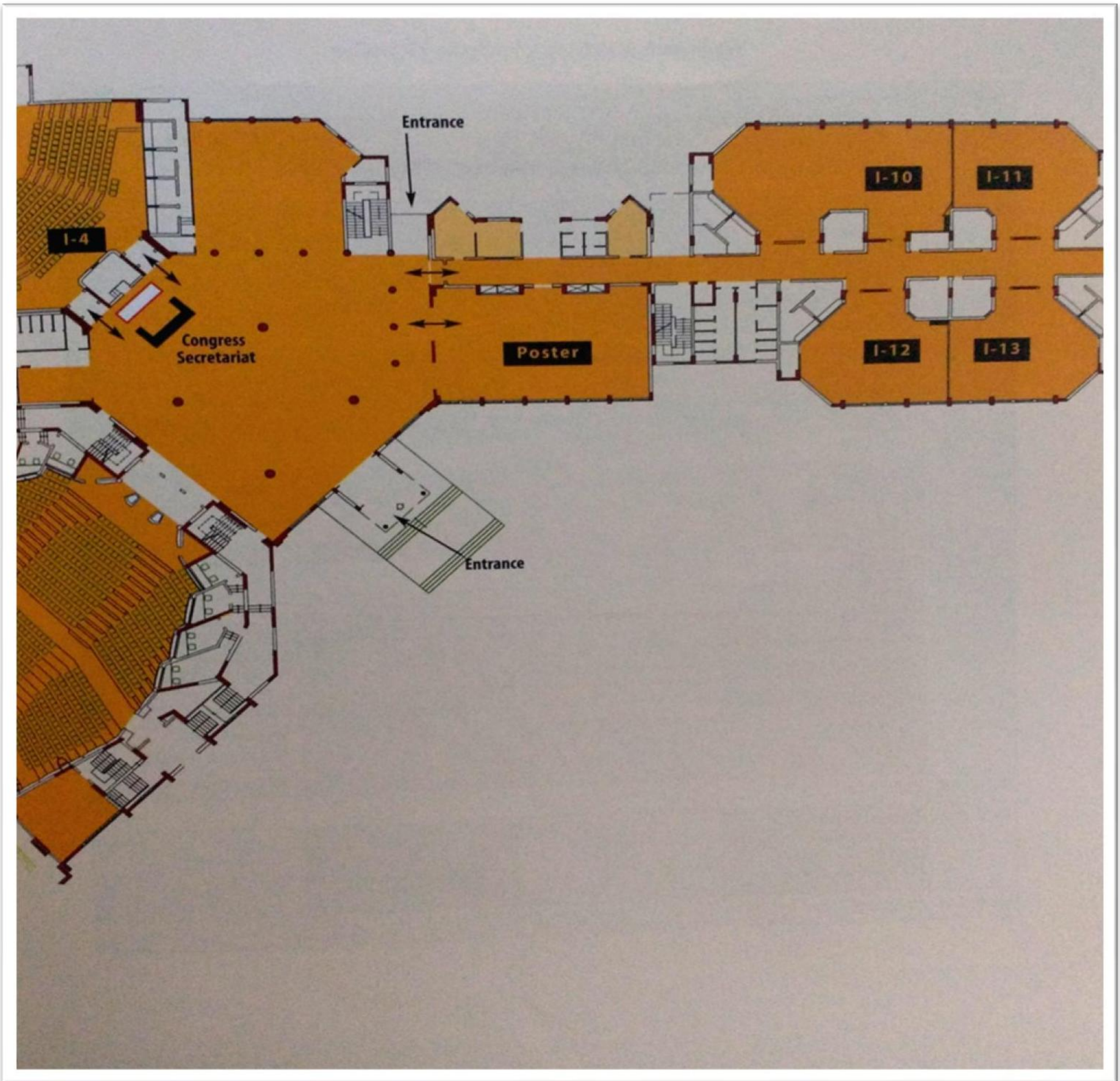

Floor plan of the Conference and Cultural Center of the University of Patras

2nd Scientific Meeting of the Tectonics Committee of the Geological Society of Greece

P R O G R A M M E

WEDNESDAY 13 JUNE

09:00- 10:00 Reception and Registration

INVITED LECTURE (HALL I-12)

Chair: Koukouvelas I., Polyzos D.

10:00 - 10:30 Welcome, Greetings and Opening Speech

10:30 - 11:00 Caputo R.: The seismic gap of northern Thessaly, Central Greece

SESSION A (HALL I-12)
THE MOVRI Mtn EARTHQUAKE

Chair: Caputo R., Ganas A.

11:00 - 11:15 Papadimitriou P., Karakonstantis A., Kapetanidis V., Agalos A., Moshou A., Kaviris G., Kassaras I., Voulgaris N.: The M_w=6.4 2008 Andravida earthquake (Peloponnesus, Greece): ten years after

11:15 - 11:30 Karakostas V., Mirek K., Mesimeri M., Papadimitriou E., Mirek J.: The Aftershock Sequence of the 2008 Achaia, Greece, Earthquake: Joint Analysis of Seismicity Relocation and Persistent Scatterers Interferometry

11:30 - 11:45 Giannopoulos D., Sokos E., Konstantinou K., Lois A., Konstantinopoulos D.: The seismic anisotropy pattern in the epicentral area of the 2008 Movri Mtn M6.5 earthquake

11:45 - 12:00 Briole P., Elias P., Avallone A., Dimitrov D.: Co-seismic & inter-seismic ground deformations in the Movri earthquake area

12:00 - 12:15 Serpetsidaki A., Elias P., Ilieva M., Bernard P., Briole P., Deschamps A., Lambotte S., Lyon-Caen H., Sokos E., Tselentis G-A.: New Constraints from Seismology and Geodesy on the Mw=6.4 2008 Movri (Greece) Earthquake

12:15 - 12:30 Lappas S., Foumelis M., Papanikolaou I.: Tracing the impact of the 2008 Movri (Ilia) Earthquake through InSAR Ground Deformation Monitoring: implications for the ESI scale

12:30 - 12:40 Discussion

COFFEE BREAK – POSTER SESSION

SESSION B (HALL I-12)
SEISMOLOGY – DEFORMATION – TECTONICS OF WESTERN GREECE

Chair: Briole P., Papadimitriou E.

13:00 - 13:15 Rigo A., Sokos E., Giannopoulos D., Paraskevopoulos P., Germenis N., Andriopoulos G.: MAΔAM experiment: seismotectonics focus on the Gulf of Patras triple junction

13:15 - 13:30 Ganas A., Chousianitis K., Drakatos G., Argyrakis P., Papanikolaou M., Elias P., Mendonidis E., Tsimi C., Moshou A., Roukounakis N., Makaris D., Exarchos K.: A review of kinematics of west-central Greece from GNSS data: exploring the boundaries of extension and shear

13:30 - 13:45 Kazantzidou-Firtinidou D., Kassaras I., Kapetanidis V., Karakonstantis A., Papadimitriou P., Kaviris G.: The 26th March 1993 (M5.4) Pyrgos earthquake on the western segment of the Movri causative fault of the 2008 event

13:45 - 14:00 Triantafyllou I., Koukouvelas I., Papadopoulos G.: The lethal earthquake of 15th July 1909 in Chavari, Elis: a little known event

14:00 - 14:15 Haddad A., Lupi M., Planes T., Ganas A., Kassaras I.: Recent seismicity/microseismicity study in Western Peloponnese, Greece

14:15 - 14:30 Sakkas V., Lagios E., Garcia M., Bianchi M.: 25-Year Ground Deformation Studies in the broader Area of Patras Gulf based on Geodetic and Radar Interferometric techniques

14:30 - 14:40 Discussion

LUNCH BREAK – POSTER SESSION

SESSION C (HALL I-12)
REGIONAL – CASE STUDIES

Chair: Papadopoulos G., Papadimitriou P.

15:00 - 15:15 Stefanou I.: From the behavior of fault gouges to earthquake nucleation and control

15:15 - 15:30 Kassaras I., Giannaraki G., Roumelioti Z., kazantzidou-Firtinidou D., Ganas A.: Scenario based Seismic Risk assessment in Aigion for a repetition of the 15th June 1995 M6.4 earthquake

15:30 - 15:45 Mouslopoulou V., Saltogianni V., Oncken O., Nicol A., Begg J., Babeyko A., Cesca S., Moreno M.: The 2016 Mw 7.8 Kaikōura Earthquake: a rare snapshot of coseismic-slip transfer between the plate-interface and faults in the upper-crust

15:45 - 16:00 Papatheodorou G., Christodoulou D., Fakiris E., Etiope G., Ferentinos G.: The activation of the pockmark field, in Patras Gulf, triggered by the June 8, 2008 earthquake

16:00 - 16:05 Cerrone C., Ascione A., Di Donato V., Mazzoli S., Robustelli G.: Active tectonic evidence in the NE edge of the Campania Plain, southern Apennines (Italy)

16:05 - 16:20 Sakellariou D., Zavitsanou A., Tsampouraki-Kraounaki K., Rousakis G.: The interplay between active tectonics and sea-level fluctuations and their impact on the evolution of the prehistoric landscapes in the Aegean Region

16:20 - 16:35 Kiratzi A.: Source properties of engineering significance: examples from recent strong earthquakes in the Aegean Sea and the surrounding lands

16:35 - 16:45 Discussion – Conclusive Remarks

POSTER SESSION (HALL I-12)

Cerrone C., Ascione A., Di Donato V., Mazzoli S., Robustelli G.: Active tectonic evidence in the NE edge of the Campania Plain, southern Apennines (Italy)

Karamitros I., Ganas A., Chatzipetros A., Valkaniotis S., Partheniou E., Betzelou K.: Structural analysis and scarp morphology of the active Pidima fault, Messinia, Greece using Terrestrial Laser Scanner and Photogrammetry

Koukouvelas I., Litoseliti A., Zygouri V., Verroios S., Gerogiannis N., Aravadinou E., Nikolakopoulos K., Xypolias P.: Earthquake triggered rock-falls and taluses: the case of the Skolis Mtn, North Peloponnese, Greece, before and after 2008 M6.4 earthquake

Lazos I., Chatzipetros A., Pavlides S., Bitharis S., Pikridas C., Sboras S.: Ground deformation modelling, caused by the recent earthquakes of Ionian Islands, Greece

Lazos I., Chatzipetros A., Pavlides S., Bitharis S., Pikridas C.: Tectonics of the Corinth Gulf, Greece, based on primary geodetic data

Mavroulis S., Skourtsos E., Danamos G., Lekkas E.: The 2008 (June 8, Mw=6.4) Northwestern Peloponnese (Greece) earthquake: macroseismic intensity assessment using the ESI 2007 and EMS-98 scales and correlation to neotectonic structures and active faults

Mavroulis S., Dilalos S., Alexopoulos I., Vassilakis E., Lekkas E.: Multidisciplinary analysis including neotectonic mapping, morphotectonic indices, applied geophysics and remote sensing techniques for studying recently recognized active faults in Northwestern Peloponnese (Greece)

Tranos M., Georgiadis G.: Kinematic compatibility and paleostress analysis of heterogeneous fault-slip data from Kopaonik Mts. (Southern Serbia)

Brief Programme

09.00-10.00	***Reception and Registration***		
	Hall I12		***Presenter****
10.00-10.30	Greetings		
10.30-11.00	Invited Lecture		Caputo R.
	Hall I12		
11.00-12.40	Session A THE MOVRI Mtn EARTHQUAKE Oral Presentations – Discussion	*11.00-11.15*	Papadimitriou P.
		11.15-11.30	Karakostas V.
		11.30-11.45	Giannopoulos D.
		11.45-12.00	Briole P.
		12.00-12.15	Serpetsidaki A.
		12.15-12.30	Lappas S.
12.40-13.00	Coffee Break – Poster Session		
	Hall I12		
13.00-14.40	Session B SEISMOLOGY – DEFORMATION - TECTONICS OF WESTERN GREECE Oral Presentations – Discussion	*13.00-13.15*	Rigo A.
		13.15-13.30	Ganas A.
		13.30-13.45	Kassaras I.
		13.45-14.00	Triantafyllou I.
		14.00-14.15	Haddad A.
		14.15-14.30	Sakkas V.
14.40-15.00	Lunch Break – Poster Session		
	Hall I12		
15.00-16.45	Session C REGIONAL – CASE STUDIES Oral Presentations – Discussion – Closing Workshop	*15.00-15.15*	Stefanou I.
		15.15-15.30	Kazantzidou-Firtinidou D.
		15.30-15.45	Mouslopoulou V.
		15.45-16.00	Papatheodorou G.
		16.00-16.05	Cerrone C.
		16.05-16.20	Sakellariou D.
		16.20-16.35	Kiratzi A.

**As presenter is considered the first author of each contribution.*

ORGANISING COMMITTEE	
PRESIDENT	*Ioannis Koukouvelas*
VICE – PRESIDENT	*Athanassios Ganas*
SECRETARY	*Vasiliki Zygouri*
MEMBERS	*Paris Xypolias* *Charalampos Kranis* *Stelios Lozios* *Varvara Tsironi* *Emmanuel Skourtsos* *Sotirios Verroios*

The Organising Committee of the 2nd Scientific Meeting of the Tectonics Committee of the Geological Society of Greece expresses its grateful thanks to the Hellenic Petroleum for their substantial support.

Bulletin of the Geological Society
Special Publication No. 14, 2025
Publisher: Geological Society of Greece
ISBN (print) 978-618-86841-4-0
ISBN (e-book) 978-618-86841-5-7

"10 Years after the 2008 Movri Mtn M6.5 Earthquake; An earthquake increasing our knowledge for the deformation in a foreland area"

Sponsor

HELLENIC PETROLEUM